Environmental and Experimental Botany 206 (2023) 105181

Contents lists available at ScienceDirect

Environmental and Experimental Botany

journal homepage: www.elsevier.com/locate/envexpbot

Tomato *STEROL GLYCOSYLTRANSFERASE 1* silencing unveils a major role of steryl glycosides in plant and fruit development

Angel Chávez [a,1], Nidia Castillo [a,2], Joan Manel López-Tubau [a], Kostadin E. Atanasov [a,b], Emma Fernández-Crespo [c], Gemma Camañes [c], Teresa Altabella [a,b,*], Albert Ferrer [a,d,*]

[a] Plant Synthetic Biology and Metabolic Engineering Program, Centre for Research in Agricultural Genomics (CRAG), CSIC-IRTA-UAB-UB, Cerdanyola, 08193 Barcelona, Spain

[b] Department of Biology, Healthcare and the Environment, Faculty of Pharmacy and Food Sciences, University of Barcelona, 08028 Barcelona, Spain

[c] Department of Biology, Biochemistry and Environmental Sciences, School of Technology and Experimental Sciences (ESTCE), University Jaume I, 12071 Castellón de la Plana, Spain

[d] Department of Biochemistry and Physiology, Faculty of Pharmacy and Food Sciences, University of Barcelona, 08028 Barcelona, Spain

ARTICLE INFO

Keywords:
Artificial microRNA
Conjugated sterols
Gene silencing
Phytosterol metabolism
Solanum lycopersicum

ABSTRACT

Free and glycosylated sterols localize in the plant cell plasma membrane, where in combination with other lipids regulate its structure and function. The role of glycosylated sterols in regulating membrane-associated biological processes is more relevant in plants like tomato (*Solanum lycopersicum*), in which glycosylated sterols are the predominant sterols. A proper ratio of free sterols versus glycosylated sterols has proven to be essential for proper plant performance in several species, but almost nothing is known in tomato. To assess the role of glycosylated sterols in tomato plant and fruit development, we generated transgenic lines of tomato cultivar Micro-Tom expressing two different amiRNAs devised to silence *STEROL GLYCOSYLTRANSFERASE 1*, the most actively expressed of the four genes encoding sterol glycosyltransferases in this plant. *STEROL GLYCOSYLTRANSFERASE 1* gene silencing caused moderate plant dwarfism and reduced fruit size. Analysis of the profile of glycosylated sterols throughout fruit development demonstrated that the maintenance of proper levels of these compounds during the early stages of fruit development is essential for normal fruit growth, since reduced levels of glycosylated sterols trigger a transcriptional downregulatory response that affects genes involved in processes that are critical for proper fruit development, such as seed filling, cell wall extension and auxin signaling.

1. Introduction

In plants, more than 250 different sterols (phytosterols) have been described (Nes, 2011), with each species having a different sterol composition that may also vary depending on the organ and tissue type, the developmental stage, and the environmental conditions (Moreau et al., 2018; Zhang et al., 2020). Plant sterol mixtures consist of multiple minor biosynthetic intermediates and three predominant end-products, usually β-sitosterol, stigmasterol and campesterol (Moreau et al., 2002), although cholesterol is also a major sterol in some species of the *Solanaceae* family (Behrman and Gopalan, 2005). These sterols can be classified as 24-ethylsterols (stigmasterol and β-sitosterol), 24-methylsterols (campesterol), and sterols with no alkyl substituent at C24 position (cholesterol), and are formed via three different branches of the post-squalene segment of the sterol pathway (Fig. 1A). From cycloartenol, the first cyclic precursor of sterols, the pathway bifurcates in the cholesterol branch and the 24-alkylsterols branch, which again bifurcates in two branches leading to 24-methylsterols and 24-ethylsterols (De Vriese et al., 2020). Sterols occur in free form (FS) and conjugated as steryl glycosides (SG), acyl steryl glycosides (ASG) and steryl esters (SE). In SG, the C3 hydroxyl group of the sterol backbone is linked through a glycosidic bond to a sugar moiety, primarily a single glucose residue,

* Corresponding authors at: Plant Synthetic Biology and Metabolic Engineering Program, Centre for Research in Agricultural Genomics (CRAG), CSIC-IRTA-UAB-UB, Cerdanyola, 08193 Barcelona, Spain.

E-mail addresses: angel.chavezmartinez@uni-hohenheim.de (A. Chávez), nidia.castillo@bishopmuseum.org (N. Castillo), joanmanel.lopez@cragenomica.es (J.M. López-Tubau), evgenievatanassov@ub.edu (K.E. Atanasov), ecrespo@sg.uji.es (E. Fernández-Crespo), camanes@uji.es (G. Camañes), taltabella@ub.edu (T. Altabella), albertferrer@ub.edu (A. Ferrer).

[1] Present address: Plant Systems Biology Department. University of Hohenheim, 70599 Stuttgart, Germany.

[2] Present address: Pacific Center for Molecular Biodiversity, Bernice Pauahi Bishop Museum, Honolulu, USA.

https://doi.org/10.1016/j.envexpbot.2022.105181
Received 29 July 2022; Received in revised form 1 November 2022; Accepted 8 December 2022
Available online 11 December 2022

which may have a long-chain fatty acid esterified to the hydroxyl group at position C6 leading to acyl steryl glycosides (ASG). Finally, the hydroxyl group of FS can be esterified to a long-chain fatty acid producing steryl esters (SE) (Ferrer et al., 2017). FS are the common precursors of SG and SE, which are synthesized by the UDP-glucose:sterol glycosyltransferases (SGT) and the acyl-CoA/phospholipid:sterol acyltransferases (ASAT/PSAT), respectively (Fig. 1A). These enzymes have been cloned and characterized in different plants, including oat (*Avena sativa*) (Warnecke et al., 1997), *Withania somnifera* (Chaturvedi et al., 2012), cotton (*Gossypium hirsutum*) (Li et al., 2014), *Gymnena sylvestre* (Tiwari et al., 2014), Arabidopsis (*Arabidopsis thaliana*) (Banas et al., 2005; Chen et al., 2007; DeBolt et al., 2009; Stucky et al., 2015), tomato (*Solanum lycopersicum*) (Ramírez-Estrada et al., 2017; Lara et al., 2018; Burciaga-Monge et al., 2022) and rice (*Oryza sativa*) (Li et al., 2021), but the acyltransferases responsible for the synthesis of ASG have yet to be identified. FS, SG and ASG localize in the plant cell endomembrane system, primarily in the plasma membrane (PM) (Cassim et al., 2019; Boutté and Jaillais, 2020), while SE accumulate in cytoplasmic lipid bodies (Bouvier-Navé et al., 2010; Burciaga-Monge et al., 2022). The sterol species present in conjugated form are usually the same found in free form, but their relative proportions may differ (Duperon et al., 1984; Münger et al., 2015).

The relative proportions of FS finely modulate the structure, organization and biophysical properties of cell membranes (Schuler et al., 1991; Hodzic et al., 2008; Grosjean, 2015) and, consequently, their biological function and the activity of a variety of membrane-bound proteins (Carruthers and Melchior, 1986; Grandmougin-Ferjani et al., 1997; Men et al., 2008). More recently, SG and ASG have also emerged as important determinants of membrane organization and functioning. In fact, SG and ASG show the same capacity to promote order in the membranes as FS (Grosjean et al., 2015) and are enriched together with FS, sphingolipids and selected proteins in liquid-ordered phase domains reminiscent of lipid rafts, which are involved in a variety of important cell processes related to plant development and adaptation to environmental changes (Gronnier et al., 2018; Cassim et al., 2019). The role of glycosylated sterols in membrane structure and function is likely to be even more important in plants that accumulate high levels of these compounds. In contrast to most plants, in which SG and ASG are relatively minor components of the total sterol fraction, in tomato and other *Solanaceae* SG and ASG are the predominant sterols, accounting for up to 80% of the total sterol fraction (Duperon et al., 1984; Palta et al., 1993).

Although the specific role of glycosylated sterols in regulating membrane properties and functions is yet to be established, a series of forward- and reverse-genetics studies support the view that a proper ratio of glycosylated versus free sterol forms in cell membranes is crucial for normal plant cell function and overall plant performance. Reduced levels of glycosylated sterols in the Arabidopsis null mutant *ugt80A2;B1* lacking the two SGT present in this species, lead to slow growth phenotype, elongation defects in embryogenesis, defects in seed cell morphology (DeBolt et al., 2009) and the male gametophyte (Choi et al., 2014), and abnormal root epidermal cell patterning (Pook et al., 2017). Downregulation of SGTs in *W. somnifera* leads to reduced leaf area and plant height compared to control plants (Singh et al., 2016), while overexpression of WsSGTL1 improves seed germination in Arabidopsis (Mishra et al., 2013) and enhances growth of *W. somnifera* plants (Saema et al., 2016), in contrast to the stunted growth phenotype observed when this enzyme was expressed in *Nicotiana tabacum* (Pandey et al., 2014). Changes in the levels of glycosylated sterols also translate into altered defense responses against abiotic stresses, including heat, cold and salt stress (Mishra et al., 2013; Saema et al., 2016; Singh et al., 2017; Li et al., 2021), and biotic stresses such as insect attack (Mishra et al., 2017), as well as bacterial and fungal infection (Singh et al., 2016; Castillo et al., 2019). In turn, plants subjected to biotic and abiotic stresses show altered levels of glycosylated sterols (Palta et al., 1993; Whitaker, 1994; Tarazona et al., 2015; Narayanan et al., 2016) and the expression of *SGT* genes is induced (Chaturvedi et al., 2012; Ramírez-Estrada et al., 2017). Conversely, the knowledge about the function of sterols, and even less of glycosylated sterols, in fruit development is much more limited, although it has been suggested that an active synthesis of sterols is needed during the early stages of tomato fruit development to meet the increasing demand of membranes in actively dividing and expanding cells during the fruit growth phase (Narita and Gruissem, 1989). In fact, enhanced sterol levels during the early development of melon fruits were correlated with larger fruit size (Kobayashi et al., 2002), and expression of the catalytic domain of melon 3-hydroxy-3-methylglutaryl Coenzyme A reductase (HMGR) in tomato fruit pericarp cells induced cell division and elongation leading also to bigger fruits (Kobayashi et al., 2003).

To investigate in more detail the function of glycosylated sterols in tomato plant and fruit development, we generated transgenic tomato plants (cv Micro-Tom) with reduced SG levels due to amiRNA-mediated silencing of *SlSGT1*, which is the most actively expressed member of the tomato *SlSGT* gene family (Ramírez-Estrada et al., 2017). We demonstrate that normal SG levels are essential for proper tomato fruit growth and provide evidence that reduced levels of SG in early developing fruits induce a transcriptional downregulatory response affecting mainly genes related to seed filling, cell wall metabolism, and hormone signaling.

(A)

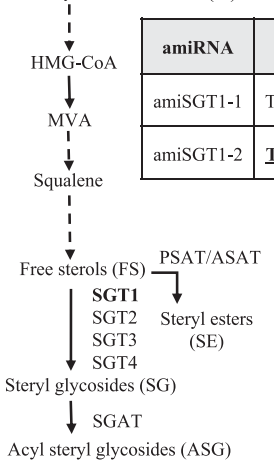

(B)

amiRNA	Sequence	mRNA position	Hybridization energy	Mismatch position
amiSGT1-1	TTAGTGAAAACGTACTTGCT**C**	1835-1855	36.70 (Kcal/mol)	1 (21)
amiSGT1-2	**T**TCTCGTAAGTTCCATC**G**CGG	209-229	40.87 (Kcal/mol)	2 (1,18)

(C)

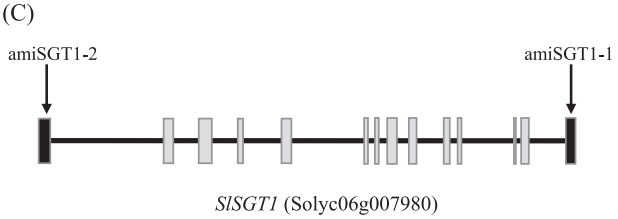

Fig. 1. Silencing of tomato *SlSGT1* gene expression using amiRNA technology. (A) Simplified scheme of the free and conjugated sterols biosynthetic pathway. Solid arrows represent single enzymatic steps and dashed arrows represent multiple enzymatic reactions. The reactions catalyzed by sterol glycosyltransferases (SGT), sterol glycosyl acyltransferase (SGAT), and sterol acyltransferases (PSAT and ASAT) are indicated. (B) Main features of the amiRNAs devised for *SlSGT1* gene silencing. (C) Structure of the *SlSGT1* gene showing the relative position of exons (boxes) and introns (solid line). Arrows indicate the position of sequences in first and last exons (black boxes) of *SlSGT1* targeted by the two amiRNAs used in this study.

2. Materials and methods

2.1. Plant growth conditions

Tomato (*S. lycopersicum*, cv Micro-Tom) seeds were directly sown 5 mm deep in pots (13 cm diameter x 10 cm height) containing a mixture of peat (Klasmann TS2), perlite and vermiculite (3:1:1). Pots were placed in plastic trays filled with water up to 1 cm high, and covered with plastic film to maintain 100% relative humidity (RH). Trays were placed in a greenhouse under long-day conditions (16 h light/8 h dark) at 26–28°C (day) and 22–24°C (night). Sunlight was used with an automatic minimum LED light supply of 200 μmol $m^{-2}s^{-1}$ to guarantee the 16 h light every day. The plastic film cover was drilled for air circulation and to favor acclimatization to greenhouse conditions once cotyledons appeared (approximately 1 week after planting the seeds), and was removed when the first true leaves were fully expanded.

2.2. Generation of pre-amiRNA expression vectors and plant transformation

The amiRNA sequences amiSGT1–1 and amiSGT1–2 were designed using the Web MicroRNA Designer (http://wmd3.weigelworld.org/cgi-bin/webapp.cgi) (Ossowski et al., 2008). The transgenes encoding the amiSGT foldbacks were generated by overlapping PCR using pRS300 plasmid (Addgene plasmid #22846) as a template and primers shown in Supplementary Table S1. The amplified fragments were cloned into pDONR221 using Gateway BP clonase II enzyme mix (Invitrogen) and sequenced in the resulting pENTRY clones to exclude amplification artifacts. Three entry clones bearing the 35SCaMV promoter, the pre-amiRNA constructs, and the *Agrobacterium tumefaciens* nopaline synthase terminator (tNOS) were recombined with pKGW,0 destination vector (Plant Systems Biology, Ghent, Belgium) in a single multisite recombination reaction using Gateway LR clonase II enzyme mix (Invitrogen). The obtained binary plasmids were transferred to *A. tumefaciens* strain GV3101::pMP90 and the resulting strains were used to transform tomato (cv. Micro-Tom) cotyledons (Fernández et al., 2009). The presence of the transgenes in kanamycin-resistant tomato plants (T0) was checked by PCR amplification of a 1137-bp fragment extending from the 3′ region of the NPTII gene to the 5′-end of the amiSGT foldback coding sequence, and a 686-bp fragment extending from the 5′-end of the amiSGT foldback coding sequence to the 3′ end of the tNOS, using primers shown in Supplementary Table S1 and leaf genomic DNA obtained using the cetyltrimethyl ammonium bromide (CTAB) method (Richards et al., 1994). The transgene copy number in the positive T0 plants was determined by qPCR (Yang et al., 2005) using tomato *LAT52* (Solyc10g007270) as endogenous single-copy reference gene, *NPTII* as target transgene, and primers shown in Supplementary Table S1. Seeds from the T0 plants were collected and segregating homozygous T1 plants harboring a single copy of each transgene were selected for characterization.

2.3. Real-time PCR expression analysis

RNA was isolated from ground frozen leaf and fruit tissue (100 mg) with the Maxwell® RSC Plant RNA Kit and the Maxwell® RSC Instruments (Promega). The cDNA samples were synthesized from 1 μg of DNA-free RNA using the NZY First-Stand cDNA Synthesis kit (NZYtech), and their integrity was assessed by PCR amplification of an actin cDNA fragment using primers shown in Supplementary Table S2. Real-time PCR analyses were performed in a LigthCycler 480 Real Time PCR System (Roche) in a total volume of 20 μl containing 10 μl LightCycler 480 SYBR Green I Master (Roche Diagnostics), 0.6 μl forward primer (0.3 μM), 0.6 μl reverse primer (0.3 μM), 6.8 μl water and 2 μl cDNA (50 ng), using the following run protocol: 95°C for 10 min followed by 40 cycles of 95°C for 10 s, 60°C for 30 s, and a final step at 4°C. The raw PCR data from LightCycler software 1.5.0 were used in the analysis. For efficiency determination of primer pairs, a standard curve of six serial dilution points ranging from 6.25 to 200 ng was performed in triplicate. Dissociation curves for PCR products were checked for non-specific amplification. Assays were performed in three biological replicates, with three technical replicates for each biological replicate. The amount of target mRNAs was normalized using the tomato actin gene (Solyc03g078400) as a reference and primers indicated in Supplementary Table S2. Normalized transcript abundances were calculated as follows: ΔCt = Ct target – Ct reference, and the fold-change value was calculated using the $2^{-\Delta Ct}$ expression (Livak and Schmittgen, 2001).

2.4. Construction of transgenic lines harboring a proSlSGT1::GUS gene fusion and histochemical analysis of GUS activity

A 2420 bp fragment of the *SlSGT1* 5′-flanking region (positions −2422 to −2 relative to the first nucleotide of the ATG codon) was amplified by PCR using proSlSGT1-fw and proSlSGT1-rv primers (Supplementary Table S1), genomic DNA as a template, and PhusionTM High-Fidelity DNA polymerase (Thermofisher Scientific). The amplified fragment was purified and cloned into pDONR207 to create ENTRY clone pDONR207-proSGT1. The *SlSGT1* promoter fragment was transferred into the pDestination binary vector pGWB433, yielding binary plasmid proSlSGT1::GUS. The fusion between the *SlSGT1* promoter fragment and the GUS coding sequence was confirmed by sequencing, and tomato (cv. Micro-Tom) cotyledons were transformed as indicated in Section 2.2. For histochemical analysis of GUS activity, tomato fruit slices were incubated at 37°C in 5-bromo-4-chloro-3-indolyl-β-D-glucuronide (X-Gluc) substrate solution (1 mg/mL X-Gluc, 100 mM sodium phosphate (pH 7.0), 10 mM EDTA, 0.1% (v/v) Triton X-100, 0.2 mM potassium ferrocyanide, and 0.2 mM potassium ferricyanide). Samples were washed with 0.1 M sodium phosphate buffer (pH 7.0), cleared with 70% ethanol and photographed.

2.5. Gene expression analysis by RNA-Seq

Three independent pools of 10 fruits were collected from each tomato genotype at 9 DAA. Samples were frozen and ground in liquid nitrogen, and total RNA was isolated as described above. The quality and quantity of RNA samples was assessed using a Bioanalyzer Expert 2100 Instrument (Agilent Technologies). The cDNA libraries were prepared according to Illumina protocols from 3 μg of total RNA per sample and sequenced using an Illumina HiSeq 2500 machine (2 ×75 bp paired-end sequencing). The quality of the reads was checked with FastQC software (http://www.bioinformatics.bbsrc.ac.uk/projects/fastqc/). Low quality bases and adapters were removed from raw reads with BBDuk (minimum base quality 25 and minimum length 35 bp). The reads were aligned against the *Solanum lycopersicum* (SL3.0) reference genome with STAR aligner (version 2.5.2b). FeatureCounts (version 1.5.1) was used to calculate gene expression values as raw fragments counts (annotation version ITAG 3.2). Normalization was applied to the raw fragment counts by using the Trimmed Mean of M-values (TMM) and Fragments per Kilobase Million (FPKM) normalization. All the statistical analyses were performed with R using the packages HTSFilter, edgeR and NOISeq. No expressed genes and the ones showing high variability were removed. The HTSFilter package was chosen for this scope, which implements a filtering procedure for replicated transcriptome sequencing data based on a Jaccard similarity index. Sequencing data can be obtained from the Sequence Read Archive (SRA) database under the accession numbers SRR18577213, SRR18577214 and SRR18577215.

2.6. Sterol analysis

For leaf sterol analysis, the third and fourth leaves of three independent groups of 10 one-month-old plants per genotype were collected, pooled, frozen in liquid nitrogen, and stored at − 80°C until use. For fruit sterol analysis, flowers of 20 plants per genotype were tagged on the day

of anthesis and pools of 20 fruits were harvested at 15 (green), 30 (mature green), 32 (breaker), and 36 (red) days after anthesis (DAA). Fruits were frozen in liquid nitrogen and stored at − 80ºC. Frozen tissue samples (25–30 μg) were grinded to a fine powder, lyophilized, and suspended in 3 mL of a chloroform-methanol (2:1) mixture containing 5 μg of each of the following internal standards: cholestanol (FS), cholestanyl palmitate (ES), cholestanyl-β-D-glucoside (SG), and palmitoyl-β-D-glucosylcholestanol. After vortexing and sonication for 10 min at room temperature in an ultrasonic water bath, 1.5 mL of 0.9% (w/v) NaCl were added to facilitate phase separation. The organic phase was recovered by centrifugation at 3000 x g for 5 min at room temperature and transferred to a new tube. The remaining aqueous phase was extracted again with 3 mL of chloroform-methanol (2:1), and the two organic extracts were mixed together and evaporated to dryness. The dried residue was dissolved in 150 μl of chloroform-methanol (2:1), and the four sterol fractions were separated by TLC using precoated silica gel PLC 60 F254 plates (20 ×20 cm) (Merck, Darmstadt) and dichloromethane-methanol-acetic acid (92:8:2) as a mobile phase. A mixture of the free and conjugated sterol standards was also applied onto the TLC plates as markers. For visualization of the sterol fractions, plates were sprayed with a 0.01% primuline (Sigma-Aldrich) solution and illuminated with a UV lamp. The different fractions were scraped from the silica plates for subsequent sterol extraction. For the acid hydrolysis of SG and ASG, 1.5 mL of a 2 N HCl methanolic solution was added to the silica powder, while the SE fraction was saponified in 1.5 mL of 7.5% KOH methanolic solution. After incubation at 85°C for 2 h, the hydrolysis reactions were quenched with 1.5 mL of 0.9% (w/v) NaCl. The FS moieties released from SG, ASG and SE were extracted twice with 3 mL of n-hexane. The hexanic phases were collected by centrifugation at 3000 x g for 5 min at room temperature, mixed and evaporated to dryness. Sterols were derivatized by adding 50 μl of Bis (trimethylsilyl) trifluoroacetamide (BSTFA) (Regis Technologies) followed by a 20 min incubation at 80°C. After evaporation to dryness, sterols were dissolved in 50 μl of isooctane and analyzed by GC-MS, using an Agilent 7890 A gas chromatograph equipped with a Sapiens-X5MS capillary column (30 m x 0.25 mm × 0.25 mm) (Tecnokroma analítica) coupled with a 5975 C mass spectrometer (Agilent). The retention index obtained for n-propyl benzene and 1-heptanol was 953.0 and 967.8, respectively. Helium 99,99% pure was used at 1 mL/min flux. Oven program was from 70ºC to 255ºC at a ramp rate of 20ºC/min (hold for 40 min), then to 300ºC at a ramp rate of 3ºC/min (hold for 5 min). The injector was set at 270ºC, transfer line at 230ºC and ion source at 150ºC. The solvent delay was set at 23 min. The scanning mass range was from 50 to 550 amu. Data acquisition and processing were done by Agilent MSD ChemStation software, and quantification of sterols was based on the relative peak area of cholestanol. Peak integration was performed manually and the annotation of each peak was carried out using the NIST mass spectral library (NIST08).

2.7. Photosynthetic parameters

Tomato plants were grown for 4 weeks in pots filled with sterile vermiculite in a growth chamber under long day conditions (16 h light/8 h dark), at 26ºC (day) and 22ºC (night), 200 μmol $m^{-2}s^{-1}$ light intensity and 60% relative humidity. Determinations were carried out *in situ* on the apical part of leaves of the same age grown under standard conditions or subjected to salt stress. In the latter case, plants were irrigated with 100 mM NaCl for 24 h, with 200 mM NaCl for an additional 24 h, and finally with 400 mM NaCl for 6 days. The gas exchange analysis was carried out using a portable open system infrared gas analyzer (LI-6800 portable photosynthesis system, LI-COR, USA) under ambient CO_2 and humidity. The photosynthetic rate (μmol CO_2 $m^{-2}s^{-1}$), transpiration rate (mol H_2O $m^{-2}s^{-1}$) and stomatal conductance (mol H_2O $m^{-2}s^{-1}$) were calculated from 3 measures per leaf on 3 different plants. Experiments were repeated 3 times (n = 9).

2.8. Statistical analysis

Quantitative experimental data were subjected to one-way analysis of variance (ANOVA) or two-way ANOVA in the case of time-course gene expression analysis shown in Fig. 11, followed by Tukey's multiple comparisons test at $\alpha < 0.05$, using GraphPad Prism v8.0.2 (La Jolla, California, USA).

3. Results

3.1. Generation of tomato SlSGT1-silenced lines

To investigate the biological function of SG in tomato, we generated transgenic tomato plants (cv Micro-Tom) expressing two different amiRNAs (amiSGT1–1 and amiSGT1–2) specifically devised to down-regulate the expression of the *SlSGT1* gene (Fig. 1B). These amiRNAs targeted sequences within first (amiSGT1–2) and last (amiSGT1–1) exons of *SlSGT1* (Fig. 1C). Two independent homozygous lines harboring a single copy of the *amiSGT1–1* and *amiSGT1–2* transgenes, referred to as amiSGT1–31.2 and amiSGT1–61.1, respectively, were selected for further characterization. *SlSGT1* expression analysis revealed a strong reduction of SlSGT1 mRNA levels in leaves and fruits at different developmental stages of both mutant lines compared to their wild type (wt) counterparts (Fig. 2). On the contrary, no major changes in the mRNA levels of the remaining members of the *SlSGT* gene family were observed neither in leaves nor in fruits of amiSGT1 lines compared to wt plants (Supplementary Fig. S1). All these results demonstrated that both amiRNAs were highly specific and effective in silencing *SlSGT1* expression in tomato plant leaves and fruits.

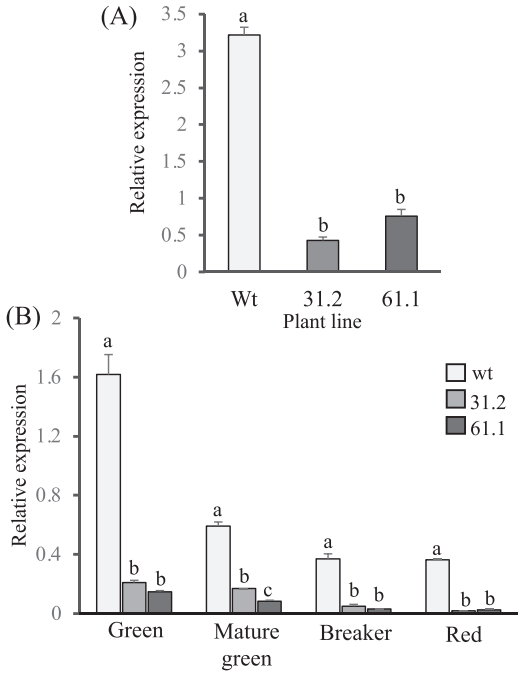

Fig. 2. SlSGT1 mRNA levels in leaves and fruits of amiSGT1 plants. RT-qPCR analyses were performed using RNA samples from the third and fourth leaves of one-month-old plants (A) and fruits at the indicated developmental stages (B). The mRNA levels of the actin gene were used to normalize SlSGT1 transcript levels. Data are presented as mean ± SEM from three leaf biological replicates per genotype with three technical replicates each (n = 9) and three technical replicates per genotype, using pooled pericarp tissue from 15 fruits at each stage (n = 3). In leaves (A) and at each fruit developmental stage (B) different letters (a-c) indicate significant differences among wt and amiSGT1 lines.

3.2. Effect of SlSGT1 silencing on the profile of free and conjugated sterols in leaves and fruits

The impact of *SlSGT1* silencing on sterol metabolism was investigated in the same samples used for mRNA quantification. Total SG content in the leaves of mutant plants decreased to ~55% of the wt levels (Fig. 3, Supplementary Table S3), resulting in a reduction of the four major glycosylated sterols, albeit to varying degrees. Glycosylated stigmasterol showed the greatest reduction (~55%), followed by glycosylated β-sitosterol and campesterol (~48–43%), and glycosylated cholesterol (~25%). Surprisingly, these changes did not significantly alter neither total ASG levels nor the amounts of individual ASG species. On the contrary, FS content in both mutant lines increased to ~155% of the wt levels. The greatest increase was observed in free stigmasterol (~90%) followed by β-sitosterol and campesterol (32–45%), and cholesterol (25%). Unexpectedly, this increase in FS levels had no significant impact neither on the total content of SE (~115% of the wt levels) nor on the individual SE species, with the only exception of esterified stigmasterol, whose content increased drastically (70–100%) compared to wt levels. It is worth noting that the overall amount of membrane sterols (FS, SG and ASG) in *SlSGT1*-silenced plants was reduced only to ~90% of the wt levels, indicating that the strong negative impact of *SlSGT1* down-regulation on the SG content was largely compensated by a concomitant increase in FS.

Analysis of sterol levels in fruits revealed a steady decline of the total SG content as wt fruits developed, with an overall 72% reduction from green to red stages, contrary to mutant fruits, whose SG levels remained almost constant from green to breaker stages and then dropped sharply at the red stage (Fig. 4). This translated into marked reductions in the SG contents of amiSGT1 fruits at green (~50%), mature green (~32%) and red stages (~25–30%) compared to wt fruits, while at the breaker stage, SG levels were identical to those in control fruits (Supplementary Table S4). Interestingly, the SG profiles in wt and amiSGT1 fruits are fully consistent with the pattern of expression driven by the *SlSGT1* promoter throughout fruit development. Histochemical detection of GUS activity in fruits expressing a chimeric *proSlSGT1::GUS* gene (Fig. 5) revealed an intense and rather uniform distribution of GUS staining throughout all tissues of green fruits, which decreased gradually until fruits reached the red stage, where GUS expression was mainly concentrated in the endocarp and the funiculus. The close correlation between *SlSGT1* promoter activity and SG accumulation during fruit development was confirmed by measuring GUS mRNA levels at the different developmental stages. Particularly remarkable was the sharp decrease of both SG content and SlSGT1 mRNA levels observed when fruits enter the ripening phase (Supplementary Fig. S2). These observations strongly support a major role for SlSGT1 in fruit SG biosynthesis.

Contrary to SG levels, those of ASG remained fairly constant throughout fruit development of both wt and amiSGT1 fruits (Fig. 4, Supplementary Table S5). The main difference between the two ASG profiles is a rather uniform reduction (12–30%) of ASG in amiSGT1 fruits compared to wt fruits. As in leaves, the impaired ability to glycosylate sterols in amiSGT1 fruits also led to much higher levels of FS compared to wt fruits (Fig. 4, Supplementary Table S6), which can be accommodated without being transformed into SE, since SE levels in amiSGT1 fruits were identical to those in wt fruits at all stages of development (Fig. 4, Supplementary Table S7). Again, there was only a moderate decrease of the overall amount of membrane sterols in *SlSGT1*-silenced fruits compared to wt levels, with reductions ranging from ~5% (breaker stage) to ~25% (green stage).

3.3. Phenotype of SlSGT1-silenced lines

To assess the effect of *SlSGT1* silencing on tomato plant growth and development, we analyzed the phenotype of amiSGT1 plants. One-month-old amiSGT1 plants were on average ~25% shorter than wt plants (Fig. 6A, B), corroborating the finding that the most distal internode (fifth internode) was ~50% shorter than that of wt plants (Fig. 6C). The diameter of the distal internode was also smaller, with

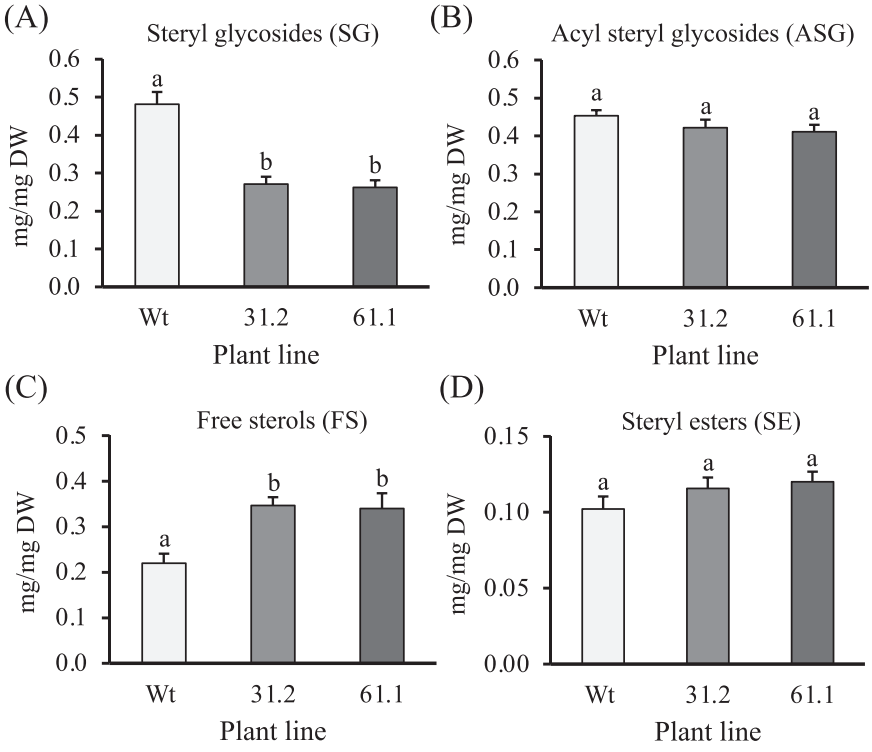

Fig. 3. Total levels of free and conjugated sterols in leaves of amiSGT1 plants. Quantification of steryl glycosides (A), acyl steryl glycosides (B), free sterols (C) and steryl esters (D) was carried out in the third and fourth leaves of one-month-old plants. Data are presented as mean ± SEM from three leaf biological replicates per genotype, with three technical replicates each (n = 9). Different letters (a-b) indicate significant differences among wt and amiSGT1 leaves.

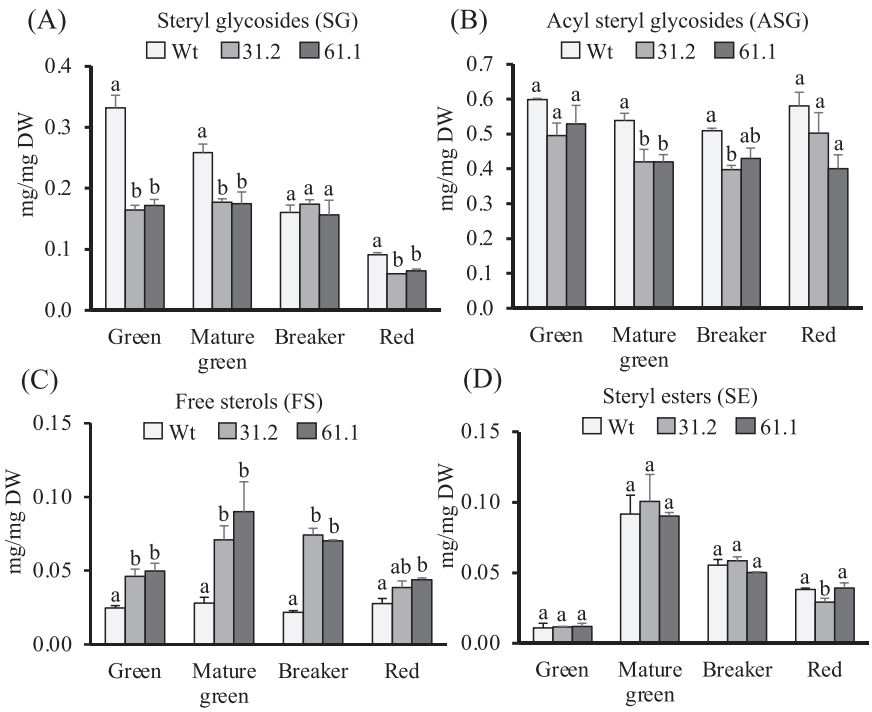

Fig. 4. Total levels of free and conjugated sterols in fruits of amiSGT1 plants. Quantification of steryl glycosides (A), acyl steryl glycosides (B), free sterols (C), and steryl esters **(D)** was carried out in fruits harvested at the indicated developmental stages. Data are presented as mean ± SEM from three biological replicates per genotype (n = 3). At each fruit developmental stage different letters (a-b) indicate significant differences among wt and amiSGT1 lines.

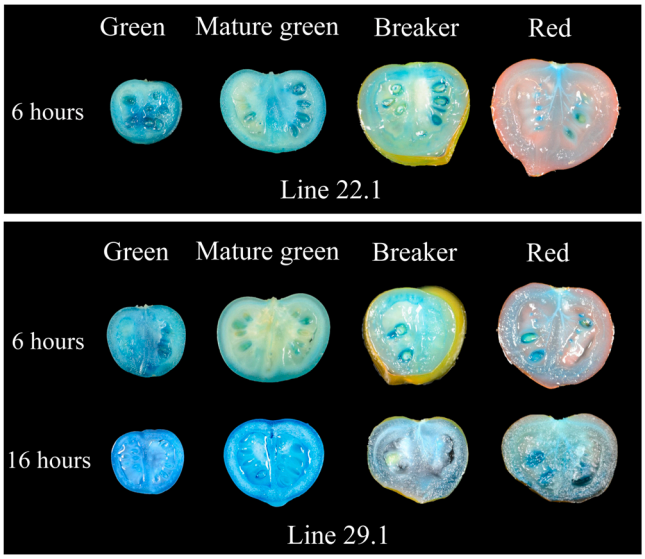

Fig. 5. Histochemical detection of GUS activity in fruits expressing a chimeric *SlSGT1:GUS* gene. The images correspond to cross-sections of representative fruits of two independent transgenic lines (22.1 and 29.1) collected at the indicated developmental stages. Green (15 DAA), mature green (30 DAA), breaker (32 DAA) and red (36 DAA). In the case of fruits from line 29.1, the images show GUS staining after incubation with the GUS substrate for 6 and 16 h.

reductions of ~35% compared to the wt (Fig. 6D). On the contrary, no significant differences were observed in the total number of leaves between mutant and wt plants, although there was a significant decrease in the foliar area, as demonstrated by the ~35% reduction in the leaf area of the third and fourth leaves of amiSGT1 plants compared to wt leaves (Fig. 6E, F). The altered profile of free and conjugated sterols also affected the photosynthetic parameters, since stomatal conductance, transpiration rate, and photosynthetic rate of amiSGT1 plants were slightly, but significantly, higher than in control plants (Fig. 7A-C). This ruled out the possibility that reduced growth of amiSGT1 plants might be due to some impairment of photosynthetic performance. No significant differences in these photosynthetic parameters were observed when plants were exposed to 400 mM NaCl (Fig. 7D-F). Interestingly, fruits of both amiSGT1 lines were also smaller (Fig. 8A) and weighed significantly less (20–40%) than wt fruits (Fig. 8B, Supplementary Table S8). The reduced fruit size was concomitant to a decrease in seed yield per fruit (Fig. 8C). On the contrary, no obvious differences were detected in fruit setting, shape or ripening. The evident correlation between depletion of SG levels and reduced fruit size indicates that proper levels of SG at the early stages of fruit development are critical for normal fruit growth but not for ripening.

3.4. Transcriptional profiling of SlSGT1-silenced fruits

To investigate the molecular mechanisms underlying the effect of reduced SG levels on fruit phenotype, global changes of gene expression in early developing amiSGT1 fruits were analyzed using an RNA-seq approach and RNA samples from three independent biological replicates (A, B, C) of amiSGT1 and wt fruits collected at 9 days after anthesis (DAA). A summary of the number of reads and mapping statistics is shown in Supplementary Table S9. Principal component analysis (PCA) based on the normalized read counts of the whole set of replicates clearly separated the amiSGT1 silenced fruits from those of wt plants in the two first dimensions, with 85.68% of the total variance at the transcript level. Thus, the samples were grouped as expected, with the only exception being sample 61.1_C, which was not included in further analysis as it did not cluster well with the corresponding group (Supplementary Fig. S3A). Differentially expressed genes (DEGs) between *SlSGT1*-silenced and wt fruits were identified, and significance was recognized only for those showing a false discovery rate (FDR) below 0.05. We found a total of 1369 downregulated genes and 524 upregulated genes in common between the two silenced lines (Supplementary Fig. S3B and Supplementary Table S10). Based on GO assignments using

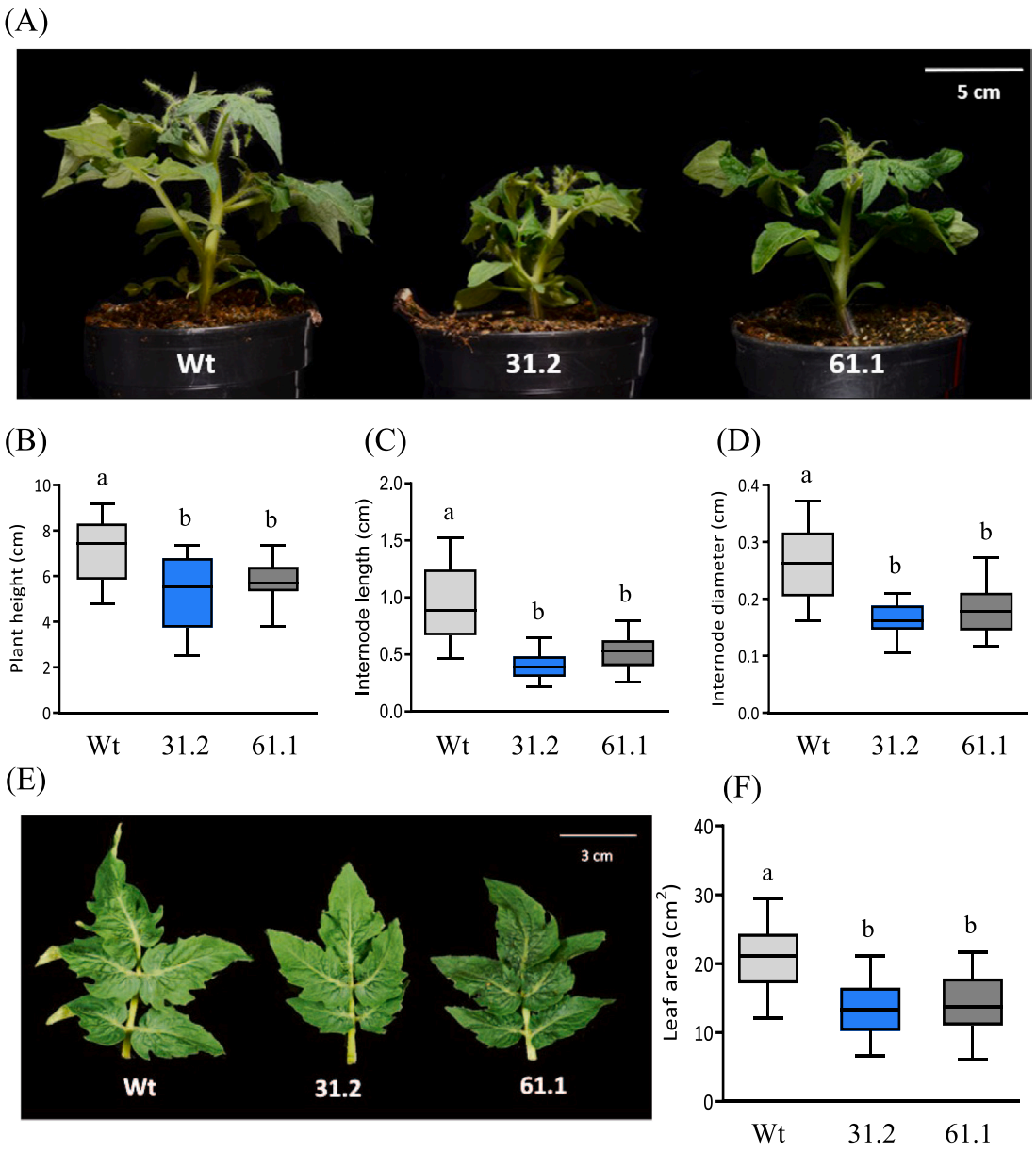

Fig. 6. Phenotypic characterization and morphometric analysis of amiSGT1 plants. (A) Representative images of one-month-old amiSGT1 and wt plants grown under greenhouse conditions. (B) Quantitative analysis of plant height to first inflorescence, (C) fifth internode length, and (D) internode diameter. (E) Representative images of the third leaf, and (F) quantitative analysis of third and fourth leaf area. Data are presented as mean ± min and max values of 35 plants per genotype. Morphometric parameters were measured using ImageJ software. Different letters (a-b) indicate significant differences.

agriGO v2.0 (http://systemsbiology.cau.edu.cn/agriGOv2/), we found 74 categories significantly overrepresented (FDR $\leq$ 0.05) based on biological process (45), molecular function (10) and cellular component (19) (Supplementary Table S11). The top 10 GO terms in these categories are shown in Supplementary Fig. S3C. Considering a $\log_2$fc $\geq$ 2 or ≤ -2, only 219 common genes were downregulated (Fig. 9 and Supplementary Table S12) and 16 upregulated (Fig. 10 and Supplementary Table S13) in both silenced lines. Thus, silencing of *SlSGT1* in green tomato fruits triggers a largely downregulatory genome-wide transcriptional response, since the number of significantly downregulated genes is about 2.5-fold (FDR<0.05) and 13.5-fold higher (log2fc $\geq$ 2 or ≤ -2) than those upregulated.

Using the function assigned on Solgenomics (https://solgenomics.net/), the 219 downregulated genes were classified into 13 categories. The most represented ones included genes encoding regulatory proteins and proteins related to metabolic processes and lipid metabolism (Fig. 9B, C and Supplementary Table S12). In the first category, the strong downregulation of the genes encoding CLE8 (Solyc05g053630) and FUS3 (Solyc02g094460) proteins was remarkable. CLE8 is a member of the CLE (CLAVATA3/EMBRYO-SURROUNDING REGION) family of plant-specific small signaling peptides involved in the developmental regulation of different organs, including fruits (Zhang et al., 2014). The expression of the Arabidopsis CLE8 homologue is restricted to the developing seeds, where it acts as a positive regulator of seed growth (Fiume and Fletcher, 2012), and tomato CLE8 expression increases sharply and continuously during the early stages of fruit development and then declines drastically when green fruit reaches maturation (Zhang et al., 2014). FUS3 is a plant-specific B3 domain transcription factor known to positively regulate the expression of genes involved in seed filling. In fact, it is one of the four master regulators controlling seed maturation (Verdier and Thompson, 2008). Interestingly, in the lipid metabolism category we identified eight genes encoding oleosins whose expression was strongly repressed in both silenced lines (Supplementary Table S12). Oleosins are the major protein constituents of

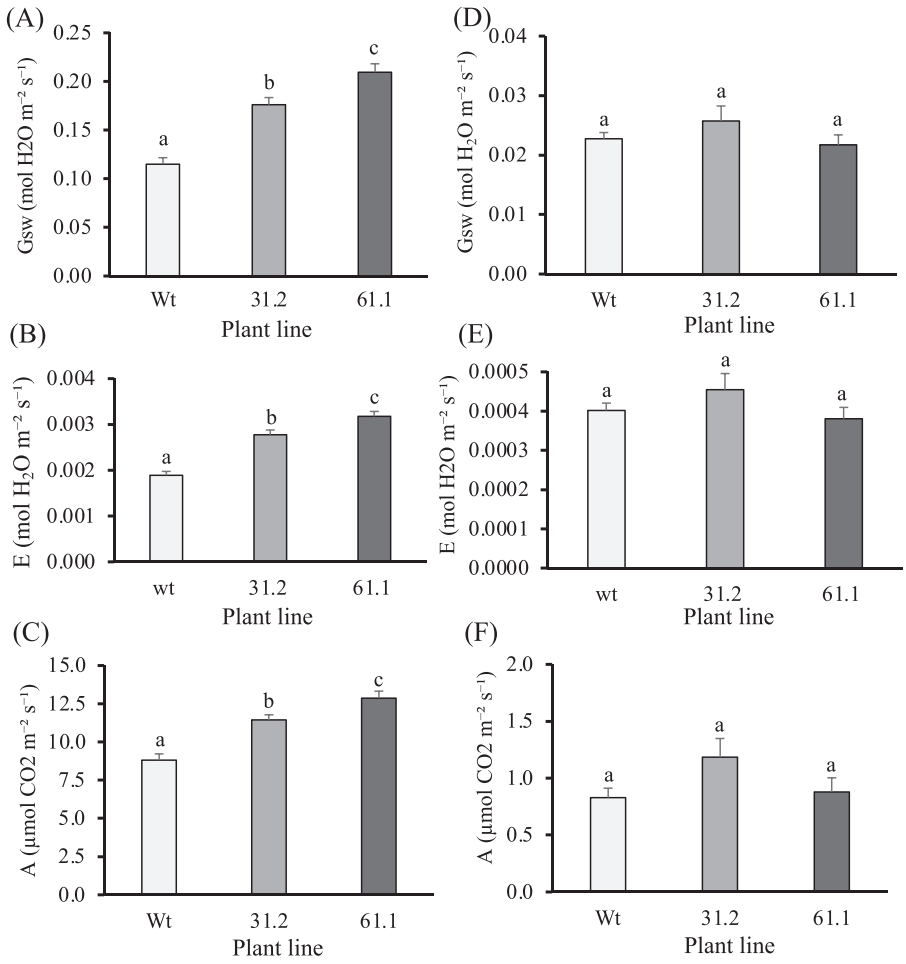

Fig. 7. Photosynthetic parameters in leaves of amiSGT1 plants. (A,D) Stomatal conductance, (B,E) transpiration rate and (C,F) photosynthetic rate of amiSGT1 and wt plants grown under standard greenhouse conditions (A-C) and exposed to 400 mM NaCl (D-F). Data are presented as mean ± SE from three biological replicates, each replicate consisting of 3 plants with three technical replicates (n = 9). Different letters (a-c) indicate significant differences.

triglyceride- and SE-rich plant oil bodies found in the cytoplasm of seeds and fruits (Liu et al., 2016). Ten more downregulated genes encoding seed storage proteins like globulins and vicilins were classified in the category of nutrient reservoir activity, eight of which were among the ten more strongly downregulated in line amiSGT1–31.2 and were also drastically repressed in line amiSGT1–61.1 (Supplementary Table S12). To validate these RNA-seq expression changes, we performed a time-course RT-qPCR expression analysis during the early stages of fruit development (4, 9 and 15 DAA) of *SlCLE8*, *SlFUS3*, and four genes encoding representative storage proteins: two oleosins and globulins 11 S and 7 S. The results were fully consistent with those obtained in the RNA-seq analysis (Fig. 11) and demonstrated a positive correlation between the reduced expression of the tomato developmental regulators CLE8 and FUS3 and the downregulation of genes encoding proteins involved in seed fillingin *SlSGT1*-silenced fruits. Thus, these results showed that seed filling is compromised as a consequence of *SlSGT1* downregulation, which may also contribute to the small fruit size phenotype given the correlation existing between normal seed development and proper fruit growth (Gillaspy et al., 1993).

Silencing of *SlSGT1* in fruits also downregulates the expression of several genes related to cell expansion (Fig. 9B, C). Although genes encoding pectinesterases, also called pectin methylesterases (PME), and expansins are the most widely represented in this group, other genes encoding proteins involved in cell wall metabolism, as pectin lyase-like protein, polygalacturonase, pectinesterase inhibitor, xylosidase, and xylanase, are also included (Table 1). Expansins are a family of proteins involved in different biological processes, including fruit development and ripening (Brummell et al., 1999; Nardi et al., 2015). The transcript levels of the tomato expansin gene *SlEXPA7* (Solyc03g115300) (Lu et al., 2016) were severely reduced in both transgenic lines, and the expression of the genes encoding EXPA20 (Solyc03g115310) and EXPB5 (Solyc07g049540) was reduced more than two-fold in both lines (Table 1). Pectinesterases catalyze the demethoxylation of pectins, which affects the biomechanical properties of the cell wall and, consequently, the cell extension (Jeong et al., 2018). The expression of *SlPME61* (Solyc10g049370) and *SlPME3* (Solyc00g170510), two genes of the broad family encoding tomato PME (Jeong et al., 2018), was reduced more than four-fold in the silenced fruits (Fig. 9 C and Supplementary Table S12), while the expression of *SlPME29* and *SlPME77* decreased more than two-fold (Table 1). On the contrary, Solyc10g038020, encoding a cellulose synthase (CesA) protein, was markedly overexpressed in the *SlSGT1*-silenced fruits (Fig. 10B, C and Supplementary Table S13). CesA catalyzes the synthesis of cellulose, which provides the major structural rigidity of the cell wall matrix (Somerville et al., 2004). The time-course expression analysis of *SlEXPA7*, *SlPME61*, and *SlCesA* genes shown in Fig. 11 confirmed the strong impact of *SlSGT1* silencing on the expression of different cell wall-related genes, suggesting that defects in cell wall biogenesis and structure may hamper cell elongation and contribute to the reduced fruit size observed as a result of *SlSGT1* downregulation.

Interestingly, among the 219 genes downregulated in fruits of both silenced lines, we also found genes involved in the signaling pathway of auxins (four genes of the Gretchen Hagen 3 (GH3) gene family) and GA (GAST1) (Table 1 and Supplementary Table S12). Moreover, the

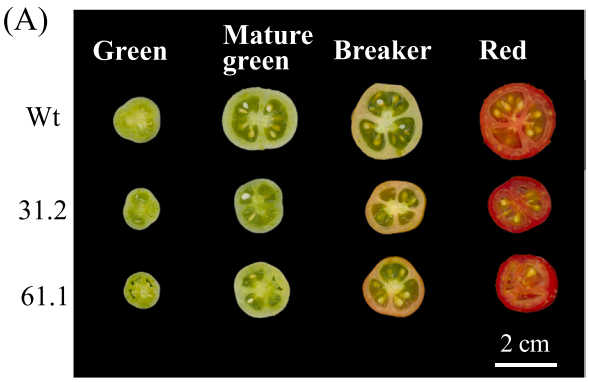

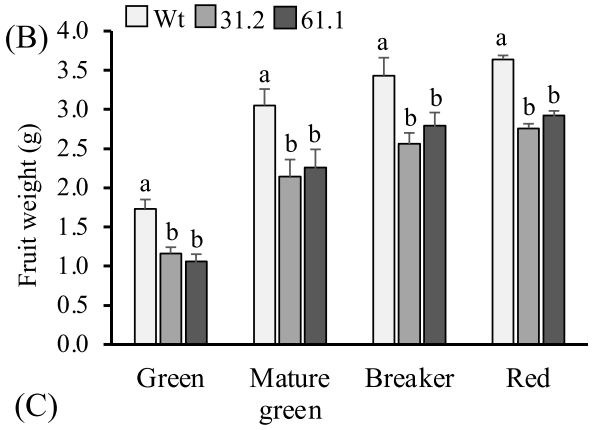

(C)

Average seed number per fruit		
Wt	Line 31.2	Line 61.1
13.0 ± 1.4 (a)	7.2 ± 0.88 (b)	9.0 ± 0.7 (b)

Fig. 8. Phenotypic characterization of fruits from amiSGT1 plants. (A) Representative cross-section images and (B) weight quantification of fruits collected from amiSGT1 and wt plants at the indicated developmental stages. Green (15 DAA), mature green (30 DAA), breaker (32 DAA) and red (36 DAA). Data are presented as mean ± SEM from 35 fruits at each developmental stage per genotype. (C) Average seed number in fruits of amiSGT1 plants. Data are presented as mean ± SEM from 35 fruits. At each fruit developmental stage (B) and in Table C different letters (a-b) indicate significant differences among wt and amiSGT1 lines.

expression of genes encoding small auxin-induced RNAs (SAURs), auxin/indole-3-acetic acid (Aux/IAA) and auxin-response factor (ARF) proteins was reduced more than two-fold in *SlSGT1*-silenced fruits (Table 1). The same was observed for three genes encoding two GA-regulated proteins and one GRAS family transcription factor (Table 1). These data suggest that the small fruit size phenotype observed as a result of decreased SG levels could be mediated through the auxin and GA signaling pathways. In fact, these are the primary regulatory phytohormones during the early stages of fleshy fruit development (Quinet et al., 2019; Fenn and Giovannoni, 2021).

4. Discussion

4.1. Downregulation of SlSGT1 alters the balance of free and glycosylated sterols

The expression of two different amiRNAs targeting the tomato (Micro-Tom) *SlSGT1* gene (Fig. 1) caused a strong downregulation of the SlSGT1 mRNA levels in both leaves and fruits (Fig. 2) without substantially affecting the expression of the remaining members of the *SlSGT* gene family (Supplementary Fig. S1), and led to the same morphological, biochemical and molecular alterations, thus confirming that the phenotypes of amiSGT1 plants can be specifically attributed to the silencing of *SlSGT1* expression. The downregulation of *SlSGT1* caused a pronounced reduction in SG levels of leaves and fruits at different developmental stages, with the only exception being fruits at the breaker stage, which showed normal levels of SG (Figs. 3, 4 and Supplementary Table S3, S4). The low transcriptional activity of the *SlSGT1* promoter observed at this stage of fruit development (Supplementary Fig. S2) could explain this observation. Either way, the close correlation between the SG content and the activity of the *SlSGT1* promoter throughout wt fruit development (Supplementary Fig. S2), along with the impact of *SlSGT1* downregulation on SG levels in the leaves and fruits of amiSGT1 plants (Fig. 4 and Supplementary Table S4), strongly support a major role of SlSGT1 in tomato SG metabolism. In this regard, a detailed analysis of SG profiling data in leaves and fruits of amiSGT1 plants revealed that all major glycosylated sterols are depleted to a greater or lesser extent in both organs (Supplementary Table S3–7), which is consistent with previous results showing that SlSGT1 is able to glycosylate different sterol species both *in vitro* and *in vivo* (Ramírez-Estrada et al., 2017). In fact, substrate promiscuity seems to be a common feature of plant SGTs. The Arabidopsis UGT80A2 and UGT80B1 SGTs can also glycosylate all major sterols (Stucky et al., 2015) and the *W. somnifera* SGTL1 and SGTL4 isozymes have the capacity to interact not only with a variety of sterols but also with steroidal lactones (Pandey et al., 2015). It remains to be established whether the differential reduction in the levels of the main SG species caused by *SlSGT1* silencing is due to differences in SlSGT1 affinity for its FS substrates and/or in substrate availability, since the levels of the different FS are clearly distinct (Supplementary Table S3, S6).

Interestingly, the metabolic effects of *SlSGT1* downregulation are not restricted to SG. In leaves, the reduction of SG levels to about half those in control plants resulted in a two-fold increase of total FS, while neither ASG nor ES levels were significantly altered (Fig. 3 and Supplementary Table S3). A similar metabolic response was observed in fruits, where the decline in SG also led to an increase in FS, although in this case ASG levels were also affected. Indeed, a small but significant decrease in ASG levels was observed at all stages of development, although there was no clear quantitative correlation with the corresponding changes in SG levels (Fig. 4). Such a weak or even lack of correlation between the total contents of SG and ASG was also observed in the seeds of the Arabidopsis *ugt80* mutants (Stucky et al., 2015). Thus, it appears that in certain tissues and/or developmental stages, SG levels might not be limiting for normal ASG production despite being the direct precursors of ASG. On the other hand, it is also worth noting that the increase of total FS caused by the reduction in SG content did not translate into a concomitant increase in total SE levels, neither in leaves nor in fruits (Fig. 4). Only esterified stigmasterol increased significantly in leaves, but the impact on the total content of ES was negligible because of the low proportion of esterified stigmasterol in the conjugated sterol fraction (Supplementary Table S3). The lack of correlation between increased levels of FS and normal levels of SE was unexpected, since membrane FS levels are tightly regulated to avoid the toxicity associated with excess FS (Shimada et al., 2019). Indeed, previous studies showed that a forced increase in the flux of the sterol pathway leads to enhanced levels of SE while the content of FS remains essentially unaltered (Wilkinson et al., 1994; Schaller et al., 1995; Harker et al., 2003). A plausible hypothesis is that excess FS in leaves and fruits of amiSGT1 plants is not converted into non-harmful SE because they can be readily accommodated in the existing cell membranes, partly compensating for the reduction in SG levels, since the total content of membrane sterols (FS, SG, and ASG) in both leaves and fruits of amiSGT1 plants is still lower than in the corresponding wt organs, with values ranging from ~75–95% those in control plants. In any case, there is an important disturbance of the balance between the different membrane sterol species that very likely

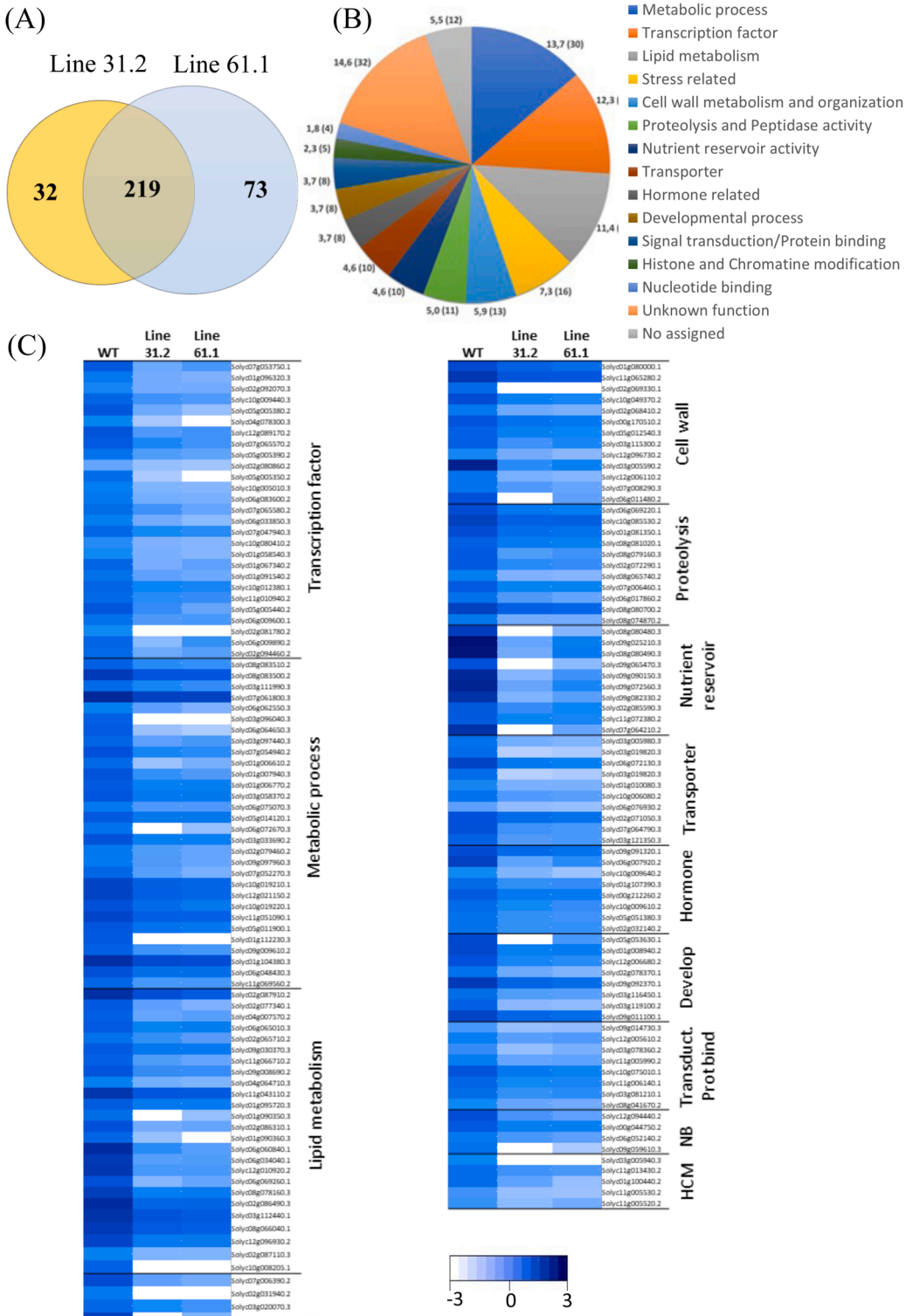

Fig. 9. Genes downregulated in fruits of amiSlSGT1 plants considering a log2 fold change (fc) ≤ 2. (A) Venn diagram showing the number of downregulated genes in 9DAA fruits of the *SlSGT1*-silenced lines 31.2 and 61.1. (B) Classification of the 219 commonly downregulated genes in fruits of the two amiSGT1 lines based on gene ontology (AgriGov2) and the assigned function in the Solgenomics Network (https://solgenomics.net/). The number of each category indicates the percentage of genes in that category relative to the 219 downregulated genes, and numbers in brackets represent the number of genes included in each category. (C) Heatmaps showing expression changes of the downregulated genes with an assigned function. The colour scale shows the levels of gene expression as log2-scaled values of fragments per kilobase million (FPKM) (log2 FPKM), with values ranging from -3 (lower expression, white) to $+3$ (higher expression, dark blue), as indicate at the bottom. HCM = Histone and chromatin modification; NB = Nucleotide binding.

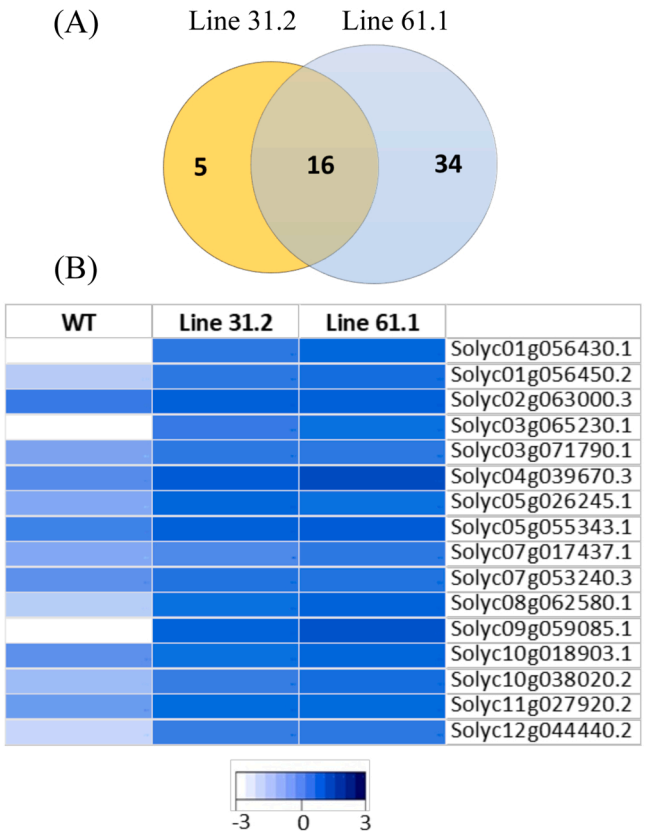

Fig. 10. Genes upregulated in fruits of the amiSGT1 plants considering a log2 fold change (fc) ≤ 2. (A) Venn diagram showing the number of upregulated genes in 9DAA fruits of the *SlSGT1*-silenced lines 31.2 and 61.1. (B) Heatmap showing expression changes of the 16 commonly upregulated genes in fruits of the two amiSGT1 lines. The colour scale shows the levels of gene expression as log2-scaled values of fragments per kilobase million (FPKM) (log2 FPKM), with values ranging from − 3 (lower expression, white) to + 3 (higher expression, dark blue), as indicate at the bottom.

alters their biophysical properties.

4.2. Changes in the expression of genes involved in seed filling, cell extension and auxin signaling mediate the reduced fruit size phenotype of amiSGT1 plants

The morphological phenotypes of amiSGT1 plants and fruits are fully consistent with the reduced leaf area and plant height caused by the downregulation of SGTs in *W. somnifera* plants (Singh et al., 2016), and the drastic arrest of tomato fruit growth observed when sterol biosynthesis is blocked during the early stages of fruit development (Narita and Gruissem, 1989). Our results reinforce the hypothesis that fruit growth inhibition was a direct consequence of sterol depletion (Narita and Gruissem, 1989) and demonstrate that normal tomato fruit growth is specifically dependent on fruits having proper levels of SG in the early stages of development.

To shed some light on the molecular mechanisms underlying the small size of amiSGT1 tomato fruits, we performed a global transcriptomic study in fruits at 9 DAA. This analysis revealed that *SlSGT1* silencing triggers a wide downregulatory transcriptional response since the number of repressed genes was much higher than that of upregulated ones (Figs. 9, 10). One of the most prominent responses was a strong downregulation of a high number of genes encoding storage proteins (globulins and vicilins) and oleosins, which on the other hand does not compromise normal SE accumulation (Fig. 4D), and proteins that regulate seed development, such as the small secretory signaling peptide CLE8 and the transcriptional regulators FUS3 and ABI3 (Supplementary Table S12). CLE8 is a positive regulator of seed growth (Fiume and Fletcher, 2012) while ABI3 and FUS3 activate the expression of genes involved in seed development (Verdier and Thompson, 2008), including those coding for oleosins (Kirik et al., 1996; Carbonero et al., 2017). It is thus conceivable that the expected lower accumulation of storage proteins during the seed filling may prevent correct seed development and, consequently, that of the fruit, since seed number and distribution determines the size and shape of many fruits (Gillaspy et al., 1993; Srivastava and Handa, 2005). Indeed, after fertilization, seeds produce auxin and GA that promote fruit growth (Dorcey et al., 2009) and determine its final size by regulating the expression of cell cycle and expansion genes (Ozga et al., 1992; Gillaspy et al., 1993; Serrani et al., 2007; Pattison and Catalá, 2012). Thus, low seed production induced by *SlSGT1* downregulation (Fig. 8C) may explain, at least in part, the reduced fruit size phenotype of the *SlSGT1*-silenced fruits (Fig. 8A and B).

Our transcriptome expression analysis also showed a strong downregulation of several genes coding for proteins related to cell expansion, including PMEs, expansins (Table 1), and a tomato homologue of the Arabidopsis homeobox-leucine zipper protein ATHB12 (Fig. 9 C and Supplementary Table S12), which induces the expression of different genes related to cell expansion (Hur et al., 2015). The highest PME activity has been detected in tomato green fruits cell types involved in cell expansion and elongation (Jeong et al., 2018). Expansins induce cell wall extension (Cosgrove et al., 2002) and some members of the tomato expansin gene family are expressed in fruits where they play a role in fruit development and ripening (Brummell et al., 1999; Nardi et al., 2015; Lu et al., 2016). On the contrary, the expression of a gene encoding CesA was strongly upregulated in the *SlSGT1*-silenced fruits (Fig. 11 and Supplementary Table S13). An increase of cellulose synthesis would limit normal cell growth by reducing cell wall extensibility since cellulose provides rigidity to the cell wall (Somerville, 2004). Hence, it is tempting to speculate that all these changes may compromise normal cell wall loosening and extension in the mutant fruit cells, which may limit their expansion capacity, thus also contributing to the observed *SlSGT1*-silenced fruit size reduction.

Our hypothesis that depletion of SG levels due to *SlSGT1* silencing has a negative impact on the cell expansion process is further supported by the results of the time-course expression analysis of selected genes encoding proteins involved in seed filling (CLE8, FUS3, two oleosins and two globulins) and cell wall metabolism (SlXPA7, PME61, CesA). This analysis confirmed the RNA-seq results and demonstrated that the transcriptional response of the selected genes at 9 DAA was maintained or even enhanced at 15 DAA, when fruit growth is mainly due to cell expansion (Gillaspy et al., 1993), while it was almost completely absent at 4 DAA (Fig. 11) when cell division predominates, with the only exception being the early upregulation of the genes encoding CesA (Fig. 11). The observation that only one cell cycle-related gene (Solyc12g087900) encoding CiclynD2 was also markedly repressed in the amiSlGT1 fruits (Supplementary Table S10) reinforce the idea that the small size of tomato amiSGT1 fruits can be attributed to defects in cell expansion rather than to cell division. Interestingly, most of the cell expansion genes repressed in response to *SlSGT1* silencing (Table 1) are regulated by the auxin and GA signaling pathways. The possible involvement of auxin in determining the reduced size of amiSGT1 fruits is further supported by the downregulation of several genes of the three families of early auxin responsive genes (Aux/IAA, GH3, SAUR) (Table 1) that mediate the role of this hormone in processes such as cell division, extension and differentiation (Abel and Theologies, 1996). The promoters of these genes contain the auxin-responsive element (AuxRE) (Guilfoyle et al., 1998) recognized by the auxin response factors (ARFs) that mediate the hormone response. All members of the tomato ARF family have been suggested to play a role in reproductive tissue development (Zouine et al., 2014), and one of them, SlARF18, which is expressed in green and mature fruits, was also downregulated in our mutant fruits (Table 1). Interestingly, the AuxRE is also present in the

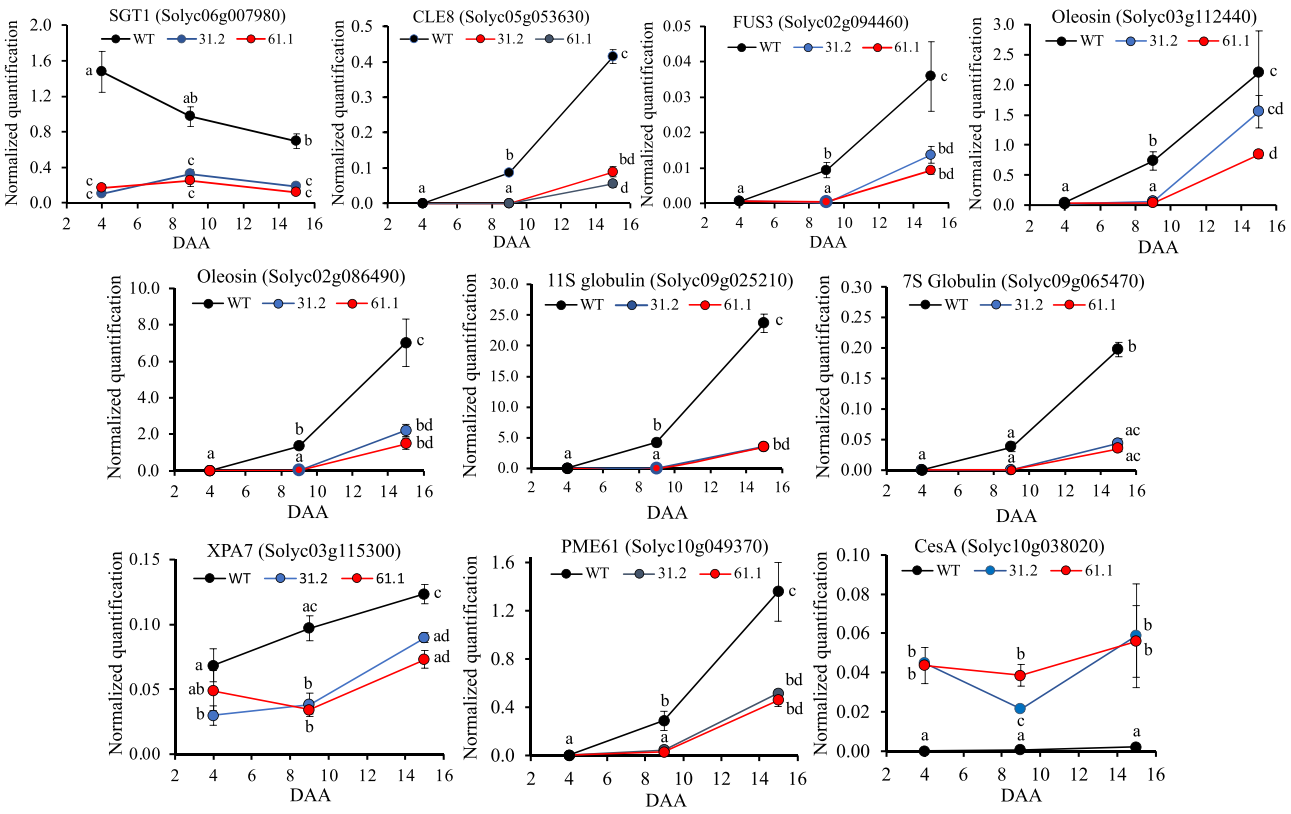

Fig. 11. Time-course expression analysis of selected genes involved in seed filling and cell wall metabolism in early developping fruits of amiSGT1 plants. The mRNA levels of the indicated genes were quantified by RT-qPCR using RNA from fruits collected at 4, 9 and 15 days after anthesis (DAA) and the primer pairs shown in Supplemental Table 2. The mRNA levels of the actin gene were used to normalize transcript levels. Data are presented as mean ± SEM from three replicates per sample using pooled tissue from 15 fruits at each stage (n = 3). Different letters (a-d) indicate significant differences.

FUS3 and *ABI3* gene promoters (Hagen and Guilfoyle, 2002), suggesting that these genes may also be auxin responsive. The above early auxin responsive genes also regulate the auxin-GA interactions (Fenn and Giovannoni, 2021). In fact, four GA-related genes are also downregulated in *SlSGT1*-silenced fruits (Table 1). However, the higher number and the relevant role of the auxin-related genes downregulated in these fruits compared to the GA-related (Table 1) leads us to propose that the auxin pathway plays a primary role in determining the reduced size of amiSlSGT1 fruits. This hypothesis is consistent with the established link between membrane lipid metabolism and composition and the hormonal control of plant developmental programs (Boutté and Jaillais, 2020), particularly between sterols and auxin synthesis, transport, signaling and response (Souter et al., 2002; Men et al., 2008; Zhang et al., 2016; Short et al., 2018; Wang et al., 2021). So far it is not possible to define the mechanistic connection between changes in the membrane sterol composition due to *SlSGT1* silencing and the developmental alteration of the amiSGT1 fruits, but it is reasonable to assume that it might be due to the impact of changes in the balance between, and within, free and glycosylated sterol pools on membrane organization and dynamics. Indeed, it is widely accepted that changes in the relative proportions of sterols influence membrane biophysical properties due to their different membrane ordering capacity (Schuler et al., 1991; Hodzic et al., 2008; Grosjean et al., 2015), and thus alter the trafficking, sorting, interactions and activity of a variety of membrane proteins involved in basic cellular functions (Carruthers and Melchior, 1986; Grandmougin-Ferjani et al., 1997; Men et al., 2008; Yang et al., 2013; Grison et al., 2015; Pook et al., 2017), including hormonal control of plant growth and development (Souter et al., 2002), although the underlying molecular mechanisms are still largely unknown. In this context, the amiSGT1 tomato mutants reported in this work represent a valuable tool for future studies aimed at unraveling the biochemical and molecular mechanisms by which changes in the homeostasis of membrane sterols influence plant growth and development.

5. Concluding remarks

The results of this study highlight the essential role of sterols in normal tomato plant and fruit development, and show that reduced levels of glycosylated sterols in early developing fruits trigger a transcriptional regulatory response that affects genes involved in critical processes for proper fruit development, such as seed filling, cell wall expansion, and auxin signaling. Overall, these results expand our current knowledge on the biological role of sterol homeostasis in plant species like tomato, where glycosylated sterols are the predominant form of membrane sterols.

Author contributions

AC and NC performed most of the experimental work. JML-T obtained and characterized the transgenic lines expressing the *SlSGT1:GUS* chimeric gene. KEA contributed to RNA-seq data management and analysis. EF-C and GC performed the measurements of photosynthetic parameters. TA and AF conceived the research, managed and supervised the project, and wrote the manuscript. All the authors analyzed data.

Declaration of Competing Interest

The authors declare that they have no known competing financial interests or personal relationships that could have appeared to influence the work reported in this paper.

Table 1
Genes related to cell wall metabolism and organization, and auxin and gibberellin signaling downregulated (FC ≤ 2) in the two amiSlSGT1-silenced lines (31.2 and 61.1).

	FC 31.2	FC 61.1	Annotation
CELL WALL METABOLISM and ORGANIZATION			
Solyc10g049370.2	-7.36	-8.34	Pectinesterase (SolycPME61)
Solyc00g170510.2	-4.24	-5.08	Pectinesterase (SolycPME3)
Solyc12g098340.2	-5.56	-2.90	Pectinesterase (SolycPME77)
Solyc02g083830.2	-2.44	-3.96	Pectinesterase (SolycPME29)
Solyc02g069330.1	-15.78	-15.84	Pectinesterase inhibitor (SolycPMEI8)
Solyc02g068410.2	-6.30	-7.44	Pectin lyase-like superfamily protein
Solyc07g056290.2	-3.58	-4.38	Polygalacturonase
Solyc03g115300.2	-7.04	-5.98	Expansin SlEXPA7
Solyc03g115310.1	-3.62	-4.26	Expansin SlEXPA20
Solyc07g049540.2	-3.70	-3.64	Expansin SlEXPB5
Solyc03g121680.2	-5.60	-5.02	Cell wall invertase
Solyc07g008290.3	-5.38	-7.24	O-fucosyltransferase family protein
Solyc10g074490.2	-3.32	-3.90	O-fucosyltransferase family protein
Solyc03g019750.3	-3.82	-4.96	Alpha-1 4-glucan-protein synthase
Solyc06g076170.3	-2.06	-2.72	Glucan endo-1,3-β-glucosidase
Solyc11g044910.2	-3.26	-3,26	β-D-xylosidase 1
Solyc01g105500.3	-2.74	-2.76	Endo-1,4-β-xylanase
AUXINS			
Solyc10g009640.2	-6.08	-8.38	Auxin-responsive GH3 family protein
Solyc01g107390.3	-4.72	-4.62	Auxin-responsive GH3 family protein
Solyc00g212260.2	-4.28	-4.50	Auxin-responsive GH3 family protein
Solyc10g009610.2	-4.14	-4.98	Auxin-responsive GH3 family protein
Solyc07g014620.1	-3.40	-3.96	Small auxin up-regulated RNA63 (SAUR)
Solyc06g053830.3	-3.10	-2.52	Auxin-regulated IAA7
Solyc01g096070.3	-2.34	-2.36	Auxin Response Factor 18 (ARF18)
GIBBERELLINS			
Solyc06g007920.2	-14.22	-11.28	Gibberellin-regulated family protein (GAST1)
Solyc12g089300.2	-3.08	-3.90	Gibberellin-regulated protein 2
Solyc06g007890.3	-2.30	-3.00	Gibberellin-regulated family protein
Solyc04g014830.2	-2.00	-2.28	GRAS family transcription factor (SlGRAS14)

Data Availability

Data will be made available on request.

Acknowledgements

We thank Pilar Fontanet for her invaluable help in the generation of the tomato transgenic lines characterized in this study, and the CRAG greenhouse staff members for the maintenance of plants. We also thank Pilar García (ESCTE, University Jaume I) for critical reading of the manuscript, and Ricardo Aiese (Sequentia Biotech) for helping in the RNA-seq data analysis. This work was supported by grants AGL2017-88842-R and PID2021-126591OB-I00 funded by MCIN/AEI/10.13039/501100011033, FEDER, a way of making Europe (Spain), and grant 2017SGR710 from the Generalitat de Catalunya. This work was also supported by grants CEX2019-000902-S funded by MCIN/AEI/10.13039/501100011033 (Spain) and by the CERCA Programme of the Generalitat de Catalunya.

Appendix A. Supporting information

Supplementary data associated with this article can be found in the online version at doi:10.1016/j.envexpbot.2022.105181.

References

Abel, S., Theologies, A., 1996. Early genes and auxin action. Plant Physiol. 111, 9–17. https://doi.org/10.1104/pp.111.1.9.

Banas, A., Carlsson, A.S., Huang, B., Lenman, M., Banas, W., Lee, M., Noiriel, A., Benveniste, P., Schaller, H., Bouvier-Navé, P., Stymne, S., 2005. Cellular sterol ester synthesis in plants is performed by an enzyme (phospholipid:sterol acyltransferase) different from the yeast and mammalian acyl-CoA:sterol acyltransferases (https://doi.). J. Biol. Chem. 280, 34626–34634. https://doi.org/10.1074/jbc.M504459200.

Behrman, E.J., Gopalan, V., 2005. Cholesterol and plants. J. Chem. Educ. 82, 1791–1793. https://doi.org/10.1021/ed082p1791.

Boutté, Y., Jaillais, Y., 2020. Metabolic cellular communications: feedback mechanisms between membrane lipid homeostasis and plant development (https://doi.). Dev. Cell 54, 171–182. https://doi.org/10.1016/j.devcel.2020.05.005.

Bouvier-Navé, P., Berna, A., Noiriel, A., Compagnon, V., Carlsson, A.S., Banas, A., Stymne, S., Schaller, H., 2010. Involvement of the phospholipid sterol acyltransferase 1 in plant sterol homeostasis and leaf senescence (https://doi.). Plant Physiol. 152, 107–119. https://doi.org/10.1104/pp.109.145672.

Brummell, D.A., Harpster, M.H., Dunsmuir, P., 1999. Differential expression of expansin gene family members during growth and ripening of tomato fruit (https://doi.). Plant Mol. Biol. 39, 161–169. https://doi.org/10.1023/a:1006130018931.

Burciaga-Monge, A., López-Tubau, J.M., Laibach, N., Deng, C., Ferrer, A., Altabella, T., 2022. Effects of impaired steryl ester biosynthesis on tomato growth and developmental processes (https://doi.). Front. Plant Sci. 13, 984100. https://doi.org/10.3389/fpls.2022.984100.

Carbonero, P., Iglesias-Fernández, R., Vicente-Carbajosa, J., 2017. The AFL subfamily of B3 transcription factors: evolution and function in angiosperm seeds (https://doi.). J. Exp. Bot. 68, 871–880. https://doi.org/10.1093/jxb/erw458.

Carruthers, A., Melchior, D.L., 1986. How bilayer lipids affect membrane-protein activity (https://doi.). Trends Biochem. Sci. 11, 331–335. https://doi.org/10.1016/0968-0004(86)90292-6.

Cassim, A.M., Gouguet, P., Gronnier, J., Laurent, N., Germain, V., Grison, M., Boutté, Y., Gerbeau-Pissot, P., Simon-Plas, F., Mongrand, S., 2019. Plant lipids: Key players of plasma membrane organization and function (https://doi.). Prog. Lipid Res. 73, 1–27. https://doi.org/10.1016/j.plipres.2018.11.002.

Castillo, N., Pastor, V., Chávez, A., Arró, M., Boronat, A., Flors, V., Ferrer, A., Altabella, T., 2019. Inactivation of UDP-glucose sterol glucosyltransferases enhances Arabidopsis resistance to *Botrytis cinerea* (https://doi.). Front. Plant Sci. 10, 1162. https://doi.org/10.3389/fpls.2019.01162.

Chaturvedi, P., Mishra, M., Akhtar, N., Gupta, P., Mishra, P., Tuli, R., 2012. Sterol glycosyltransferases-identification of members of gene family and their role in stress in *Withania somnifera* (https://doi.). Mol. Biol. Rep. 39, 9755–9764. https://doi.org/10.1007/s11033-012-1841-3.

Chen, Q., Steinhauer, L., Hammerlindl, J., Keller, W., Zou, J., 2007. Biosynthesis of phytosterol esters: identification of a sterol O-acyltransferase in Arabidopsis (https://doi.). Plant Physiol. 145, 974–984. https://doi.org/10.1104/pp.107.106278.

Choi, H., Ohyama, K., Kim, Y.-Y., Jin, J.-Y., Lee, S.B., Yamaoka, Y., Muranaka, T., Suh, M. C., Fujioka, S., Lee, Y., 2014. The role of Arabidopsis ABCG9 and ABCG31 ATP binding cassette transporters in pollen fitness and the deposition of steryl glycosides on the pollen coat (https://doi.). Plant Cell 26, 310–324. https://doi.org/10.1105/tpc.113.118935.

Cosgrove, D.J., Li, L.C., Cho, H.T., Hoffmann-Benning, S., Moore, R.C., Blecker, D., 2002. The growing world of expansins (https://doi.). Plant Cell Physiol. 43, 1436–1444. https://doi.org/10.1093/pcp/pcf180.

De Vriese, K., Pollier, J., Goossens, A., Beeckman, T., Vanneste, S., 2020. Dissecting cholesterol and phytosterol biosynthesis via mutants and inhibitors. J. Exp. Bot. 72, 241–253. https://doi.org/10.1093/jxb/eraa429.

DeBolt, S., Scheible, W.R., Schrick, K., Auer, M., Beisson, F., Bischoff, V., Bouvier-Nave, P., Carroll, A., Hematy, K., Li, Y., Milne, J., Nair, M., Schaller, H., Zemla, M., Somerville, C., 2009. Mutations in UDP-glucose:sterol glucosyltransferase in Arabidopsis cause transparent testa phenotype and suberization defect in seeds. Plant Physiol. 151, 78–87. https://doi.org/10.1104/pp.109.140582.

Dorcey, E., Urbez, C., Blázquez, M.A., Carbonell, J., Perez-Amador, M., 2009. Fertilization-dependent auxin response in ovules triggers fruit development through the modulation of gibberellin metabolism in Arabidopsis (https://doi.). Plant J. 58, 318–332. https://doi.org/10.1111/j.1365-313X.2008.03781.x.

Duperon, R., Thiersault, M., Duperon, P., 1984. High level of glycosylated sterols in species of Solanum and sterol changes during the development of the tomato. Phytochemistry 23, 743–746. https://doi.org/10.1016/S0031-9422(00)85016-5.

Fenn, M.A., Giovannoni, J.J., 2021. Phytohormones in fruit development and maturation (https://doi.). Plant J. 105, 446–458. https://doi.org/10.1111/tpj.15112.

Fernández, A.I., Viron, N., Alhagdow, M., Karimi, M., Jones, M., Amsellem, Z., Sicard, A., Czerednik, A., Angenent, G., Grierson, D., May, S., Seymour, G., Eshed, Y., Lemaire-Chamley, M., Rothan, C., Hilson, P., 2009. Flexible tools for gene expression and silencing in tomato (https://doi.). Plant Physiol. 151, 1729–1740. https://doi.org/10.1104/pp.109.147546.

Ferrer, A., Altabella, T., Arró, M., Boronat, A., 2017. Emerging roles for conjugated sterols in plants (https://doi.). Prog. Lipid Res. 67, 27–37. https://doi.org/10.1016/j.plipres.2017.06.002.

Fiume, E., Fletcher, J.C., 2012. Regulation of Arabidopsis embryo and endosperm development by the polypeptide signaling molecule CLE8 (https://doi.). Plant Cell 24, 1000–1012. https://doi.org/10.1105/tpc.111.094839.

Gillaspy, G., Ben-David, H., Gruissem, W., 1993. Fruits: a developmental perspective (https://doi.). Plant Cell 5, 1439–1451. https://doi.org/10.1105/tpc.5.10.1439.

Grandmougin-Ferjani, A., Schuler-Muller, I., Hartmann, M.A., 1997. Sterol modulation of the plasma membrane H+-ATPase activity from corn roots reconstituted into soybean lipids (https://doi.). Plant Physiol. 113, 163–174. https://doi.org/10.1104/pp.113.1.163.

Grison, M.S., Brocard, L., Fouillen, L., Nicolas, W., Wewer, V., Dörmann, P., Nacir, H., Benitez-Alfonso, Y., Claverol, S., Germain, V., Boutté, Y., Mongrand, S., Bayer, E.M., 2015. Specific membrane lipid composition is important for plasmodesmata function

in Arabidopsis (https://doi.). Plant Cell 27, 1228–1250. https://doi.org/10.1105/tpc.114.135731.
Gronnier, J., Gerbeau-Pissot, P., Germain, V., Mongrand, S., Simon-Plas, F., 2018. Divide and rule: plant plasma membrane organization (https://doi.). Trends Plant Sci. 23, 899–917. https://doi.org/10.1016/j.tplants.2018.07.007.
Grosjean, K., Mongrand, S., Beney, L., Simon-Plas, F., Gerbeau-Pissot, P., 2015. Differential effect of plant lipids on membrane organization: Specificities of phytosphingolipids and phytosterols (https://doi.). J. Biol. Chem. 290, 5810–5825. https://doi.org/10.1074/jbc.M114.598805.
Guilfoyle, T.J., Ulmasov, T., Hagen, G., 1998. The ARF family of transcription factors and their role in plant hormone-responsive transcription (https://doi.). Cell. Mol. Life Sci. 54, 619–627. https://doi.org/10.1007/s000180050190.
Hagen, G., Guilfoyle, T., 2002. Auxin-responsive gene expression: genes, promoters and regulatory factors (https://doi.). Plant Mol. Biol. 49, 373–385. https://doi.org/10.1023/A:1015207114117.
Harker, M., Holmberg, N., Clayton, J.C., Gibbard, C.L., Wallace, A.D., Rawlins, S., Hellyer, S.A., Lanot, A., Safford, R., 2003. Enhancement of seed phytosterol levels by expression of an N-terminal truncated *Hevea brasiliensis* (rubber tree) 3-hydroxy-3-methylglutaryl-CoA reductase (https://doi.). Plant Biotechnol. J. 1, 113–121. https://doi.org/10.1046/j.1467-7652.2003.00011.x.
Hodzic, A., Rappolt, M., Amenitsch, H., Laggner, P., Pabst, G., 2008. Differential modulation of membrane structure and fluctuations by plant sterols and cholesterol (https://doi.). Biophys. J. 94, 3935–3944. https://doi.org/10.1529/biophysj.107.123224.
Hur, Y.S., Um, J.H., Kim, S., Kim, K., Park, H.J., Lim, J.S., Kim, W.Y., Jun, S.E., Yoon, E. K., Lim, J., Ohme-Takagi, M., Kim, D., Park, J., Kim, G.T., Cheon, C.I., 2015. *Arabidopsis thaliana* homeobox 12 (ATHB 12), a homeodomain-leucine zipper protein, regulates leaf growth by promoting cell expansion and endoreduplication (https://doi.). N. Phytol. 205, 316–328. https://doi.org/10.1111/nph.12998.
Jeong, H.Y., Nguyen, H.P., Eom, S.H., Lee, C., 2018. Integrative analysis of pectin methylesterase (PME) and PME inhibitors in tomato (*Solanum lycopersicum*): Identification, tissue-specific expression, and biochemical characterization (https://doi.). Plant Physiol. Biochem. 132, 557–565. https://doi.org/10.1016/j.plaphy.2018.10.006.
Kirik, V., Kölle, K., Balzer, H.-J., Bäumlein, H., 1996. Two new oleosin isoforms with altered expression patterns in seeds of the *Arabidopsis* mutant *fus3* (https://doi.). Plant Mol. Biol. 31, 413–417. https://doi.org/10.1007/BF00021803.
Kobayashi, T., Kato-Emori, S., Tomita, K., Ezura, H., 2002. Detection of 3-hydroxy-3-methylglutaryl-coenzyme A reductase protein Cm-HMGR during fruit development in melon (*Cucumis melo* L.) (https://doi.). Theor. Appl. Genet. 104, 779–785. https://doi.org/10.1007/s00122-001-0838-4.
Kobayashi, T., Kato-Emori, S., Tomita, K., Ezura, H., 2003. Transformation of tomato with the melon 3-hydroxy-3-methylglutaryl coenzyme A reductase leads to increase of fruit size. Plant Biotechnol. 20, 297–303. https://doi.org/10.5511/plantbiotechnology.20.297.
Lara, J.A., Burciaga-Monge, A., Chávez, A., Revés, M., Lavilla, R., Arró, M., Boronat, A., Altabella, T., Ferrer, A., 2018. Identification and characterization of sterol acyltransferases responsible for steryl ester biosynthesis in tomato (https://doi.). Front. Plant Sci. 9, 588. https://doi.org/10.3389/fpls.2018.00588.
Li, J., Zeng, Y., Pan, Y., Zhou, L., Zhang, Z., Guo, H., Lou, Q., Shui, G., Huang, H., Tian, H., Guo, Y., Yuan, P., Yang, H., Pan, G., Wang, R., Zhang, H., Yang, S., Guo, Y., Ge, S., Li, J., Li, Z., 2021. Stepwise selection of natural variations at CTB2 and CTB4a improves cold adaptation during domestication of japonica rice (https://doi.). New Phytol. 231, 1056–1072. https://doi.org/10.1111/nph.17407.
Li, X., Xia, T., Huang, J., Guo, K., Liu, X., Chen, T., Xu, W., Wang, X., Feng, S., Peng, L., 2014. Distinct biochemical activities and heat shock responses of two UDP-glucose sterol glucosyltransferases in cotton (https://doi.). Plant Sci. 219–220, 1–8. https://doi.org/10.1016/j.plantsci.2013.12.013.
Liu, L., Liu, H., Li, S., Zhang, X., Zhang, M., Zhu, N., Dufresne, C.P., Chen, S., Wang, Q., 2016. Regulation of BZR1 in fruit ripening revealed by iTRAQ proteomics analysis (https://doi.). Sci. Rep. 6, 33635. https://doi.org/10.1038/srep33635.
Livak, K.J., Schmittgen, T.D., 2001. Analysis of relative gene expression data using real-time quantitative PCR and the 2(-Delta Delta C(T)) method (https://doi.). Methods 25, 402–408. https://doi.org/10.1006/meth.2001.1262.
Lu, Y., Liu, L., Wang, X., Han, Z., Ouyang, B., Zhang, J., Li, H., 2016. Genome-wide identification and expression analysis of the expansin gene family in tomato (https://doi.). Mol. Genet. Genom. 291, 597–608. https://doi.org/10.1007/s00438-015-1133-4.
Men, S., Boutté, Y., Ikeda, Y., Li, X., Palme, K., Stierhof, Y.-D., Hartmann, M.-A., Moritz, T., Grebe, M., 2008. Sterol-dependent endocytosis mediates post-cytokinetic acquisition of PIN2 auxin efflux carrier polarity (https://doi.). Nat. Cell Biol. 10, 237–244. https://doi.org/10.1038/ncb1686.
Mishra, M.K., Chaturvedi, P., Singh, R., Singh, G., Sharma, L.K., Pandey, V., Kumari, N., Misra, P., 2013. Overexpression of *WsSGTL1* gene of *Withania somnifera* enhances salt tolerance, heat tolerance and cold acclimation ability in transgenic Arabidopsis plants (https://doi.). PLoS ONE 8, e63064. https://doi.org/10.1371/journal.pone.0063064.s015.
Mishra, M.K., Srivastava, M., Singh, G., Tiwari, S., Niranjan, A., Kumari, N., Misra, P., 2017. Overexpression of *Withania somnifera* SGTL1 gene resists the interaction of fungus *Alternaria brassicicola* in *Arabidopsis thaliana* (https://doi.). Physiol. Mol. Plant Pathol. 97, 11–19. https://doi.org/10.1016/j.pmpp.2016.11.003.
Moreau, R.A., Whitaker, B.D., Hicks, K.B., 2002. Phytosterols, phytostanols, and their conjugates in foods: structural diversity, quantitative analysis, and health-promoting uses. Prog. Lipid Res. 41, 457–500. https://doi.org/10.1016/S0163-7827(02)00006-1.
Moreau, R.A., Nyström, L., Whitaker, B.D., Winkler-Moser, J.K., Baer, D.J., Gebauer, S. K., Hicks, K.B., 2018. Phytosterols and their derivatives: Structural diversity, distribution, metabolism, analysis, and health-promoting uses (https://doi.). Prog. Lipid Res. 70, 35–61. https://doi.org/10.1016/j.plipres.2018.04.001.
Münger, L.H., Jutzi, S., Lampi, A.-M., Nyström, L., 2015. Comparison of enzymatic hydrolysis and acid hydrolysis of sterol glycosides from foods rich in Δ(7)-Sterols (https://doi.). Lipids 50, 735–748. https://doi.org/10.1007/s11745-015-4002-3.
Narayanan, S., Tamura, P.J., Roth, M.R., Prasad, P.V.V., Welti, R., 2016. Wheat leaf lipids during heat stress: High day and night temperatures result in major lipid alterations (https://doi.). Plant Cell Environ. 39, 787–803. https://doi.org/10.1111/pce.12649.
Nardi, C.F., Villarreal, N.M., Rossi, F.R., Martínez, S., Martínez, G.A., Civello, P.M., 2015. Overexpression of the carbohydrate binding module of strawberry expansin2 in *Arabidopsis thaliana* modifies plant growth and cell wall metabolism (https://doi.). Plant Mol. Biol. 88, 101–117. https://doi.org/10.1007/s11103-015-0311-4.
Narita, J.O., Gruissem, W., 1989. Tomato hydroxymethylglutaryl-CoA reductase is required early in fruit development but not during ripening (https://doi.). Plant Cell 1, 181–190. https://doi.org/10.1105/tpc.1.2.181.
Nes, W.D., 2011. Biosynthesis of cholesterol and other sterols (https://doi.). Chem. Rev. 111, 6423–6451. https://doi.org/10.1021/cr200021m.
Ossowski, S., Schwab, R., Weigel, D., 2008. Gene silencing in plants using artificial microRNAs and other small RNAs (https://doi.). Plant J. 53, 674–690. https://doi.org/10.1111/j.1365-313X.2007.03328.x.
Ozga, J.A., Brenner, M.L., Reinecke, D.M., 1992. Seed effects on gibberellin metabolism in pea pericarp (https://doi.). Plant Physiol. 100, 88–94. https://doi.org/10.1104/pp.100.1.88.
Palta, J.P., Whitaker, B.D., Weiss, L.S., 1993. Plasma membrane lipids associated with genetic variability in freezing tolerance and cold acclimation of Solanum species (https://doi.). Plant Physiol. 103, 793–803. https://doi.org/10.1104/pp.103.3.793.
Pandey, V., Niranjan, A., Atri, N., Chandrashekhar, K., Mishra, M.K., Trivedi, P.K., Misra, P., 2014. *WsSGTL1* gene from *Withania somnifera*, modulates glycosylation profile, antioxidant system and confers biotic and salt stress tolerance in transgenic tobacco (https://doi.). Planta 239, 1217–1231. https://doi.org/10.1007/s00425-014-2046-x.
Pandey, V., Dhar, Y.V., Gupta, P., Bag, S.K., Atri, N., Asif, M.H., Trivedi, P.K., Misra, P., 2015. Comparative interactions of withanolides and sterols with two members of sterol glycosyltransferases from *Withania somnifera* (https://doi.). BMC Bioinforma. 16, 120. https://doi.org/10.1186/s12859-015-0563-7.
Pattison, R.J., Catalá, C., 2012. Evaluating auxin distribution in tomato (*Solanum lycopersicum*) through an analysis of the PIN and AUX/LAX gene families (https://doi.). Plant J. 70, 585–598. https://doi.org/10.1111/j.1365-313X.2011.04895.x.
Pook, V.G., Nair, M., Ryu, K., Arpin, J.C., Schiefelbein, J., Schrick, K., DeBolt, S., 2017. Positioning of the SCRAMBLED receptor requires UDP-Glc:sterol glucosyltransferase 80B1 in Arabidopsis roots (https://doi.). Sci. Rep. 7, 5714. https://doi.org/10.1038/s41598-017-05925-6.
Quinet, M., Angosto, T., Yuste-Lisbona, F.J., Blanchard-Gros, R., Bigot, S., Martinez, J.-P., Lutt, S., 2019. Tomato fruit development and metabolism (https://doi.). Front. Plant Sci. 10, 1554. https://doi.org/10.3389/fpls.2019.01554.
Ramírez-Estrada, K., Castillo, N., Lara, J.A., Arró, M., Boronat, A., Ferrer, A., Altabella, T., 2017. Tomato UDP-glucose sterol glycosyltransferases: a family of developmental and stress regulated genes that encode cytosolic and membrane-associated forms of the enzyme (https://doi.). Front. Plant Sci. 8, 984. https://doi.org/10.3389/fpls.2017.00984.
Richards, E., Reichardt, M., Rogers, S., 1994. Preparation of genomic DNA from plant tissue (https://doi.). Curr. Protoc. Mol. Biol. 27, 2.3.1–2.3.7. https://doi.org/10.1002/0471142727.mb0203s27.
Saema, S., Rahman, L.U., Singh, R., Niranjan, A., Ahmad, I.Z., Misra, P., 2016. Ectopic overexpression of *WsSGTL1*, a sterol glucosyltransferase gene in *Withania somnifera*, promotes growth, enhances glycowithanolide and provides tolerance to abiotic and biotic stresses (https://doi.). Plant Cell Rep. 35, 195–211. https://doi.org/10.1007/s00299-015-1879-5.
Schaller, H., Grausem, B., Benveniste, P., Chye, M.L., Tan, C.T., Song, Y.H., Chua, N.H., 1995. Expression of the *Hevea brasiliensis* (H.B.K.) Mull. Arg. 3-hydroxy-3-methyl-glutaryl-coenzyme A reductase 1 in tobacco results in sterol overproduction (https://doi.). Plant Physiol. 109, 761–770. https://doi.org/10.1104/pp.109.3.761.
Schuler, I., Milon, A., Nakatani, Y., Ourisson, A., Albrecht, M., Benveniste, P., Hartman, M.A., 1991. Differential effects of plant ste G rols on water permeability and on acyl chain ordering of soybean phosphatidylcholine bilayers (https://doi.). Proc. Natl. Acad. Sci. USA 88, 6926–6930. https://doi.org/10.1073/pnas.88.16.6926.
Serrani, J.C., Fos, M., Atarés, A., García-Martínez, J.L., 2007. Effect of gibberellin and auxin on parthenocarpic fruit growth induction in the cv Micro-Tom of tomato. J. Plant Growth Regul. 26, 211–221. https://doi.org/10.1007/s00344-007-9014-7.
Shimada, T.L., Shimada, T., Okazaki, Y., Higashi, Y., Saito, K., Kuwata, K., Oyama, K., Kato, M., Ueda, H., Nakano, A., Ueda, T., 2019. HIGH STEROL ESTER 1 is a key factor in plant sterol homeostasis (https://doi.). Nat. Plants 5, 1154–1166. https://doi.org/10.1038/s41477-019-0537-2.
Short, E., Leighton, M., Imriz, G., Liu, D., Cope-Selby, N., Hetherington, F., Smertenko, A., Hussey, P.J., Topping, J.F., Lindsey, K., 2018. Epidermal expression of a sterol biosynthesis gene regulates root growth by a non-cell-autonomous mechanism in Arabidopsis (https://doi.). Development 145, dev160572. https://doi.org/10.1242/dev.160572.
Singh, G., Tiwari, M., Singh, S.P., Singh, S., Trivedi, P.K., Misra, P., 2016. Silencing of sterol glycosyltransferases modulates the withanolide biosynthesis and leads to compromised basal immunity of *Withania somnifera* (https://doi.). Sci. Rep. 6, 25562. https://doi.org/10.1038/srep25562.

Singh, G., Tiwari, M., Singh, S.P., Singh, R., Singh, S., Shirke, P.A., Trivedi, P.K., Misra, P., 2017. Sterol glycosyltransferases required for adaptation of Withania somnifera at high temperature (https://doi.). Physiol. Plant. 160, 297–311. https://doi.org/10.1111/ppl.12563.

Somerville, C., Bauer, S., Brininstool, G., Facette, M., Hamann, T., Milne, J., Osborne, E., Paredez, A., Persson, S., Raab, T., Vorwerk, S., Youngs, H., 2004. Toward a systems approach to understanding plant-cell walls (https://doi.). Science 306, 2206–2211. https://doi.org/10.1126/science.1102765.

Souter, M., Topping, J., Pullen, M., Friml, J., Palme, K., Hackett, R., Grierson, D., Lindsey, K., 2002. hydra mutants of Arabidopsis are defective in sterol profiles and auxin and ethylene signaling (https://doi.). Plant Cell 14, 1017–1031. https://doi.org/10.1105/tpc.001248.

Srivastava, A., Handa, A.K., 2005. Hormonal regulation of tomato fruit development: a molecular perspective. J. Plant Growth Regul. 24, 67–82. https://doi.org/10.1007/s00344-005-0015-0.

Stucky, D.F., Arpin, J.C., Schrick, K., 2015. Functional diversification of two UGT80 enzymes required for steryl glucoside synthesis in Arabidopsis (https://doi.). J. Exp. Bot. 66, 189–201. https://doi.org/10.1093/jxb/eru410.

Tarazona, P., Feussner, K., Feussner, I., 2015. An enhanced plant lipidomics method based on multiplexed liquid chromatography–mass spectrometry reveals additional insights into cold- and drought-induced membrane remodeling (https://doi.). Plant J. 84, 621–633. https://doi.org/10.1111/tpj.13013.

Tiwari, P., Sangwan, R.S., Asha, Mishra, B.N., Sabir, F., Sangwan, N.S., 2014. Molecular cloning and biochemical characterization of a recombinant sterol 3-O-glucosyl-transferase from *Gymnema sylvestre* R.Br. catalyzing biosynthesis of steryl glucosides (https://doi.). Biomed. Res. Int. 2014, 934351. https://doi.org/10.1155/2014/934351.

Verdier, J., Thompson, R.D., 2008. Transcriptional regulation of storage protein synthesis during dicotyledon seed filling (https://doi.). Plant Cell Physiol. 49, 1263–1271. https://doi.org/10.1093/pcp/pcn116.

Wang, M., Li, P., Ma, Y., Nie, X., Grebe, M., Men, S., 2021. Membrane sterol composition in Arabidopsis thaliana affects root elongation via auxin biosynthesis. Int. J. Mol. Sci. 22, 437. https://doi.org/10.3390/ijms22010437.

Warnecke, D.C., Baltrusch, M., Buck, F., Wolter, F.P., Heinz, E., 1997. UDP-glucose:sterol glucosyltransferase: cloning and functional expression in *Escherichia coli* (https://doi.). Plant Mol. Biol. 35, 597–603. https://doi.org/10.1023/A:1005806119807.

Whitaker, B.D., 1994. Lipid changes in mature-green tomatoes during ripening, during chilling, and after rewarming subsequent to chilling (https://doi.). J. Am. Soc. Hort. Sci. 119, 994–999. https://doi.org/10.21273/JASHS.119.5.994.

Wilkinson, S.C., Powls, R., Goad, J.C., 1994. The effect of excess exogenous mevalonic acid on sterol and steryl ester biosynthesis in celery (*Apium graveolens*) cell suspension cultures. Phytochemistry 37, 1031–1035. https://doi.org/10.1016/S0031-9422(00)89523-0.

Yang, H., Richter, G.L., Wang, X., Młodzińska, E., Carraro, N., Ma, G., Jenness, M., Chao, D.Y., Peer, W.A., Murphy, A.S., 2013. Sterols and sphingolipids differentially function in trafficking of the Arabidopsis ABCB19 auxin transporter (https://doi.). Plant J. 74, 37–47. https://doi.org/10.1111/tpj.12103.

Yang, L., Ding, J., Zhang, C., Jia, J., Weng, H., Liu, W., Zhang, D., 2005. Estimating the copy number of transgenes in transformed rice by real-time quantitative PCR (https://doi.). Plant Cell Rep. 23, 759–763. https://doi.org/10.1007/s00299-004-0881-0.

Zhang, X., Sun, S., Nie, X., Boutté, Y., Grison, M., Li, P., Kuang, S., Men, S., 2016. Sterol methyl oxidases affect embryo development via auxin-associated mechanisms (https://doi.). Plant Physiol. 171, 468–482. https://doi.org/10.1104/pp.15.01814.

Zhang, X., Lin, K., Li, Y., 2020. Highlights to phytosterols accumulation and equilibrium in plants: biosynthetic pathway and feedback regulation (https://doi.). Plant Physiol. Biochem. 155, 637–649. https://doi.org/10.1016/j.plaphy.2020.08.021.

Zhang, Y., Yang, S., Song, Y., Wang, Y., 2014. Genome-wide characterization, expression and functional analysis of CLV3/ESR gene family in tomato (https://doi.). BMC Genom. 15, 827. https://doi.org/10.1186/1471-2164-15-827.

Zouine, M., Fu, Y., Chateigner-Boutin, A.L., Mila, I., Frasse, P., Wang, H., Audran, C., Rousta, J.P., Bouzayen, M., 2014. Characterization of the tomato ARF gene family uncovers a multi-levels post-transcriptional regulation including alternative splicing (https://doi.). PloS One 9, e84203. https://doi.org/10.1371/journal.pone.0084203.